View metadata, citation and similar papers at core.ac.uk
brought to you by CORE
provided by Repositorio Documental de la Universidad de Valladolid

SURFACE MOVEMENT AND CASCADE PROCESSES ON DEBRIS CONES IN TEMPERATE HIGH MOUNTAIN (PICOS DE EUROPA, NORTHERN SPAIN)

Enrique Serrano[1], José Juan Sanjosé[2], Álvaro Gómez-Gutiérrez[3], Manuel Gómez-Lende[4]

[1]Department of Geography. University of Valladolid, Spain. serranoe@fyl.uva.es
[2] Department of Graphic Expression. University of Extremadura, Polytechnic School, Cáceres Spain. jjblasco@unex.es
[3] Department of Geography. University of Extremadura, Cáceres, Spain. alvgo@unex.es
[4] PANGEA Research Group. University of Valladolid. Spain. manuelglende@hotmail.com

Abstract

Debris talus is a very common landform in the temperate high mountain, so much so that it is the most representative of the periglacial and nival processes. This work studies debris cones in the Picos de Europa, an Atlantic mountain range in the north of the Iberian Peninsula. A detailed geomorphological map was prepared, fieldwork were carried out on the debris cone surface, the ground and air thermal regime was analyzed, and a five-year Terrestrial Laser Scan survey carried out. Annual volume changes on the surface of the debris cones were detected and related to active processes and sediment transfer. Two different behaviors were observed in each cone. Cone A is linear, with equilibrium between accumulation and sediment transfer, while Cone B is concave-convex denoting accumulation processes in the upper part deriving from the greater frequency of snow avalanches. Changes in morphology surpass 50 cm/year with most of the activity taking place in the highest and lowest areas. The presence and action of the ice on the debris slope are moderate or non-existent and freeze-thaw processes are only active on the walls at over 2000 m a.s.l. The main processes on debris cones are debris flow and creep related to snowcover, but sediment transfer on the slopes involves high intensity-low frequency (debris flow, avalanches) and high frequency-low intensity processes (creep, shift, solifluction and wasting).

Key words: Scree slopes, debris cones, slope processes, Terrestrial Laser Scanner, temperate high mountain

1. Introduction.

Debris talus and cones are one of the commonest landforms of temperate mountains and active ones are highly representative of the high mountain with periglacial dynamics. They have been defined as "distinctive accumulations of loose, coarse, usually angular rock debris at the foot of steep bare rock slopes" (Luckmann, 2013). The study of debris talus and cones began by analyzing the topographic position and morphology of talus and cones in cold mountain environments (Rapp, 1960; Rapp and Fairbridge, 1968) before later focusing on genetic processes, their evolution (Caine, 1974; Luckman, 1976, 1988; Kotarba et al, 1979, 1987) and processes involved in sediment and transport on debris talus and cones. Creep processes, snow avalanche relationships, rockfall, debris flows, slush avalanching, gelifluction, gravitational rolling, surface run-off and clast slideover were studied together with deposits, landforms and the internal structures defined by stratified and stocked sediments (Caine, 1969, 1974; Kirkby and Statham, 1975; Luckman, 1976, 1988; Statham, 1976; Kotarba et al., 1979; Gardner, 1979, 1983; Selby, 1983, Francou, 1988, 1991; Hinchliffe et al., 1998; Saas, 2006, Jomelli and Francou, 2000De Haas et al., 2015). A typology of taluses of high mountain environments was established, differentiating between gravitational cones dominated by rockfalls with slopes of around 35º and concave profiles; snow avalanches and boulder tongues with slopes of around 35º and concave to linear profiles; avalanche cones, characterized by slopes of between 27º and 30º segmented in two or three parts with concavity; and debris flow cones, all of them representative of the temperate high mountain (Caine, 1974; Luckman, 1988, 2013b; Selby, 1983, Francou, 1991).

The debris cones and talus dynamic in the high mountain is commonly related to periglacial environments, with higher erosion rates and sediment transfer determined by deglaciation and paraglacial environments (Ballantyne, 2002), but processes related to seasonal frozen ground

and permafrost are also important factors in the dynamic of surface debris cones (Francou, 1988, 1991; Delaloyé et al. 2003; Herz et al. 2003, Scapozza et al., 2011). Investigation on hazard assessment, rockwall retreat and rockfall supply have shown the high complexity linked to previous slides, rock type and environments, without necessarily being cold environments and freeze-related processes (Krautblatter and Dikau, 2007; Wieczorek et al. 2008; Sanders et al. 2009). Previous works have revealed the complexity of processes involved in the dynamic of debris talus and cones, in which there is a broad typology of processes taking part in sediment storage and transfer, all differentiated by environmental conditions, lithology and structure.

As described later, the study area is a glaciokarstic environment without surface drainage in which glacial erosive landforms and rockwalls are linked by debris talus and cones. The debris cones landform system can be divided in two areas, (i) the rock face, the source area for rockwalls, and (ii) the debris cones, a temporary storage where deposits are reworked prior to sediment output. The sediment cascade concept is considered to be the connection between processes and landforms in which the output of one process is the input of another. Depositional landforms work as the temporary storage of sediment output (Davies and Korup, 2010) and so the debris cone is included in the talus slopes system. Previous studies have mainly been focused on the rock wall (subsystem I) and the valley bottom (subsystem III) of the slope sediment cascade, rather than on the talus slope (subsystem II). Sediments are stored and reworked in the debris talus and cones. Denudation and rockwall retreat have been quantified and models established to understand the source area's contribution to sediment flow (e.g. Becht et al. 2005; Klaubatter and Dickau, 2007; Otto et al. 2009; Luckman, 2013a, 2013b). Klaubatter and Dickau (2007) differentiate between stages such as back weathering, filling and depletion of intermediate storage on the rock face and the final rockfall supply onto the talus slopes, but the intermediate sediment storage and processes are often

disregarded (Götz et al. 2013; Schrott and Adams, 2002; Schrott et al., 2003; Otto et al., 2009).

The aim of this work is to analyze the surface changes taking place on two cones by means of geomatic techniques and relate them to surface processes, ground temperatures, temporary storage and transfer process of sediments in temperate high mountains. The research hypothesis was that in the debris cones landform system linked to atlantics high mountain periglacial environments the frozen ground direct the main processes involved in slope sediment cascade.

2. Material and methods

2.1. Study site characteristics.

The Picos de Europa are located in the north of the Cantabrian Mountains (43°10'N/4°50'W) just 20 km from the Cantabrian Sea (Fig. 1). It is a mountain range with abrupt vertical relief and summits of up to 2700 m (Torre Cerrado, 2648 m a.s.l.) and a marked oceanic influence.

Figure 1.

The geological structure constitutes a succession of thrust faults of south vergence divided by faults (Farias, 1982) featuring as a succession of slopes related to north dip and scarped fronts to the south where the main rocky walls are located. Local and regional WNW-ESE faulting breaks up the fronts and forms successive massifs and mountain groups. The predominating rocks are limestone, the “Calizas de Montaña Formation" (Namurien to Westfalian Age), and “Picos de Europa Formation” (Westfalian-Cantabrian Age) with alternating slates, calcareous conglomerate, limestones and turbiditic sandstones of the Stephanian Age (Marquínez, 1989, 1992).

Morphostructural elements together with karstic and glacial features define the relief in the Picos de Europa. Quaternary and Little Ice Age glacial processes have shaped the massif with

106 erosive glaciokarstic landforms and accumulative glacial landforms of different Upper
107 Pleistocene glacial phases (González-Trueba, 2007a, b; Serrano et al. 2012; 2013, 2017).
108 The talus and cones studied are located in a high mountain glacio-karstic landscape with
109 periglacial and nivation processes. Active debris cones and talus are distributed between 1200
110 and 2600 m a.s.l. and are functional above 1900 m a.s.l., where seasonal frozen ground
111 environments develop (González-Trueba, 2007a; Pisabarro et al. 2017).
112 The area studied houses a set of 16 active debris cones (Figure 2) oriented to the N between
113 2350 and 2600 m a.s.l., and S, SE and SW between 1790 and 2230 m a.s.l. . (Serrano and
114 González Trueba, 2004). They are divided in the proximal, medial and distal parts as cones
115 and fans are usually defined (Leeder, 1982; Harvey, 2012). The altitude and proximity to the
116 sea favor a hyperhumid environment characterized by rainfall of around 2500 mm a^{-1} and
117 snow cover duration of around six-seven months per year above 1800 m a.s.l. (González
118 Trueba, 2007a)
119 Figure 2
120 **2.2. Applied techniques**
121 **Geomorphological mapping**
122 This is a key tool in geomorphological system analysis and the basis for understanding
123 landforms, distribution processes and relationships (Smith et al. 2011). From a 1:25.000 scale
124 geomorphological map (Serrano and González-Trueba, 2004; González Trueba, 2007b) a
125 detailed geomorphological survey of debris talus and cones in the Peña Vieja Group was
126 performed. The mapping approach to the debris cones was done by fieldwork with a GIS
127 component. Landforms and processes were digitized on orthophotographs (scale 1:5,000) and
128 a derived digital terrain model (DTM), and during the fieldwork the processes were assessed
129 manually, transferred into a GIS database and initially visualized as a geomorphological map
130 (1:10,000). The landform inventory (Serrano and González-Trueba, 2004; González-Trueba,

2007a, b) was completed by multi-temporal orthophotograph interpretation and the analysis of multidirectional shaded relief and slope grids. The map includes landform type and predominant processes (see fig. 8) of accumulation on debris cones, leading to the establishment of the spatial and altitudinal distribution of processes and the classification between active and relict landforms (Kotarba et al. 1987; Francou, 1988). The use of the sediment cascade concept (Davies and Korup, 2010) helps to organize data of the debris cones systematically, where the distinction can be made between i) sediment input into the cones, ii) sediment redistribution, and iii) output (process-specific and volumetric) (see figure 8).

A diachronic analysis of orthophotos from 1946 to 2014 revealed the large rock fall and debris flow on the SW and NW sides of Peña Vieja Group and its evolution over this 68-year period was mapped.

Coarse texture and fabric

Morphometric, granulometric and orientation analyses were performed by fieldwork in order to know the cone genesis and typology. A slope profile by grids is a very common sampling technique in the study of coarse texture and fabric analysis (Francou, 1983; Pérez, 1998). Four slope profiles were obtained from cone apex to base with 100 data points per grid, and the cone surface was sampled at nine stations along the three profiles. We established a grid of 1 m^2 and the particles inside the grid points were sampled. The area to be sampled was divided into the three areas of the cone, the proximal, middle and distal. In each area three transversally aligned grids were measured. In each grid, boulder-size between 2-24 cm on the L axis, morphometry, lithology and orientation were measured. This technique has been applied widely in the study of slope deposits and debris (Goudie, 1981; Francou, 1983; Vere and Mathews, 1985; Pérez, 1998). Data of boulder size by transect were determined by

measuring the L axis of the 50 largest clasts (> 50 cm L axis) and orientation in the field by compass and clinometer. Only the orientation data were used to establish the L axis layout.

The use of orthophotos facilitates the selection and estimation of areas with upslope imbrication, rolling fabric or sliding fabric of large boulders (over 2 meters) and the classification of coarser deposits such as snow-sliding, rockfall or creep processes, while indicating the different processes involved in the reworking of the debris cones (Kotarba et al., 1987; Francou, 1991; Pérez, 1998; Decaulne and Sæmundsson, 2010).

Thermal analysis

Data were obtained from meteorological stations in the National Park and thermal micro sensors type I-Bottom UTL-Geotest AG data-logger (with centesimal accuracy and 0.05°C error level) buried between 5 and 10 cm depth and emplaced at 1865 m a.s.l. were used to analyze the ground and air thermal regime so that thermal data around the debris cones and thermal differences between walls and deposits could be compared (Thorn et al. 1999; Pisabarro et al. 2017).

Two meteorological stations (OAPN net, Cabaña Verónica hutte -43º10´09´´N/4º50´03´´W, 2309 m a.s.l.-, and Upper station of Cablecar -43º09´08´´N/4º48´18´´W, 1853 m a.s.l.) (Figure 1), located at less than 1,000 metres from both the NW and S of the selected debris cones, were used to analyze air conditions with discontinuous data from 2011-2015. Annual Air Medium Temperatures (AAMT), the number of days with temperatures below 0ºC, the freezing index and frost cycles were calculated (Pisabarro et al. 2017).

Annual Ground Surface Medium Temperatures (AGSMT) were measured by a datalogger located just at the front of the debris cone in an area without vegetation cover that usually presents an important snow cover during the winter. The thermometers monitored ground temperatures between 4 and 6 times a day for an entire year. The data were collected between 2004 and 2007. Representative statistical parameters of temperature tendencies, phases,

freeze/thaw cycles (days with temperatures below and over 0 °C), the freezing index and temporal behaviors were estimated. Frost cycles and freezing index are the most interesting parameters because they permit the comparison of the presence of seasonal ice, depth of seasonal ice, depth of ground ice and snow cover duration related to the intensity, duration and seasonality of ice on the ground (French, 2007; Fengquing and Yanwei, 2011)

Topographic change detection by terrestrial laser scanning (TLS) survey

A TLS survey was carried out in the La Vueltona valley using a TOPCON IS Imaging Station instrument. Terrestrial laser scanning has been widely used to monitor numerous rockwalls and cliffs, glaciers and rock glaciers, to estimate small- to medium-sized volumetric changes and rockfall support (e.g. Bauer et al. 2003; Rosser et al. 2005; Sanjosé et al. 2014; Gigli et al. 2014; Fey and Wichmann, 2017).

The procedure comprised the acquisition of a sector scan from one single scan position located at 2020 m a.s.l, in front of the cones where the shadowing effects are minimal, at between 170 and 610 m from Cone 1 and 330-650 from Cone 2. As the instrument is a Total Station, each scan position was referenced to another two topographic bases to take measurements within the same system of coordinates.

Precise measurements on talus and cones were carried out for the period from 2008 to 2014. Vertical and horizontal accuracies were 1-2 cm and the long-range instrument registers points at a distance of 1000 m with an accuracy of around 2 cm. The TLS was located at an approximate distance of 300 m, 20 points s-1 were registered at distances of less than 150 m while for longer distances 1 point s-1 was captured. These points were used to generate a Digital Elevation Model (DEM) based on a Triangulated Irregular Network (TIN) surface, from which annual spatial variations of volume loss or gain were calculated. As the surface did not have any features above ground (e.g. vegetation or buildings) no filter was applied.

During the fieldwork the survey was performed twice and results compared. The heterogeneity of the clast means that when two surveys are made the points do not all coincide. The points measured are not the same in each survey and the TIN was performed using different DEMs. Therefore, when two surveys are compared the differences between the two scans is greater than 2 cm. As the medium size of boulders on the surface was considered to be ±25 cm, the estimated changes were ±25 cm due to instrument inaccuracy and the generation of the TIN. To calculate the DEM of difference (DoDs), a mesh surface was first generated for each piece of data using the TIN tool implemented within ArcGIS 10.2. These surfaces were then converted to the raster format and subtracted to produce the DoDs. Taking into account the accuracy of the coordinates for each point (≈2 cm), the DoD approach was carried out without any threshold to discriminate noise and geomorphic change. This is a commonly used conservative strategy (Wheaton et al., 2010).

The point density was obtained using a cell size of 3 x 3 m at 500 m distance, though when distances are shorter the cell is denser. Thus, the debris cone distal area has a higher density than the proximal area. The point density is sufficient for this work since the slopes do not undergo significant changes and the differences between the two TINs during the same survey are greater than 25 cm, which coincides with the medium size of boulders. The instrument measures one point every 3-4 seconds for about eight hours to obtain 4000 points per TIN. The model has a point cloud of 8000 points distributed over 16,027 m^2 for Cone A and 15,575 m^2 for Cone B.

3. Results

Processes and environment

The active debris cones are widespread from 1900 m a.s.l. and there is practically no vegetation on them. They vary in height between 170 and 319 m with slopes between 32º and

228 36º and an h/H index that is always low (Serrano and González-Trueba, 2004). Large walls
229 with little talus or cone development are predominant (Figure 3).
230 Figure 3.
231 The detailed geomorphological maps (Figure 2) reveal four dominant surface processes. The
232 main surface processes by area on the debris cones are metric to decametric debris lobes,
233 sometimes configured as block streams (Figure 2B). Debris flow, characterized by depth
234 channels of between 1 and 3 meters linked to a debris fan, is the most energetic sediment
235 transfer process in the cones analyzed. Debris flow are the second most important process by
236 area, with faster and more efficient debris transfer systems between the proximal and distal
237 parts. During the last ten years this process has been detected twice, once in each cone and in
238 different years, 2011 and 2013. Rockfalls generate boulders scattered throughout the talus
239 and cones, although the sliding fabric indicates sliding over a seasonal snow cover and creep
240 as common processes. Slide and creep are two important processes of redistribution of
241 materials on the surface of the cones. They form metric to decametric debris lobes located
242 mainly in areas with steeper slopes and made up of fine and coarse materials. They outline
243 longitudinal clast flows that move faster than the surrounding debris.
244 The debris cones studied form a part of the sediment storage and redistribution as sediment
245 transfer system toward output of the slope system. The proximal part is characterized by small
246 debris flow channels and scattered boulders with finer debris. The boulders are mainly falling
247 and rolling boulders that have come to rest at the edge of the cones, but sliding fabric is also
248 common. In the central part metric-sized debris lobes predominate supporting a homogeneous
249 slope with scattered boulders and depth debris flow channels crossing it, sometimes
250 depositing debris fan. Debris lobes are located mainly in the central and lateral areas where
251 the slope reaches maximum values and they are made up of fine and coarse materials. The
252 distal part is the most complex. Debris fans are deposited by debris flow, while boulders and

253 finer debris are scattered and boulder accumulations with sliding fabric are the most common
254 feature.
255 The thermal regime shows a large difference between the ground and the air (Table 1). In the
256 lower part of the cones and walls the AAMT is around 2.4ºC higher than in the upper areas
257 with an increase in the Freezing Index from moderate to intense (208 points) and 20 more
258 freeze/thaw cycles. The ground temperature, recorded at 1865 m a.s.l., shows higher AGMT,
259 a very low Freezing Index and hardly any freeze/thaw cycles. The ground thermal regime
260 indicates a strong dependence on the snow cover, such that only in years with a thin or short-
261 lasting snow cover did temperatures reach -1ºC/-2ºC (Pisabarro et al. 2017).
262 The duration of the snow cover over the seven years studied was highly variable, between two
263 months in 2012 and seven months in 2013, as is common in the wet and moderately cold high
264 mountain (AAMT, 6ºC at 1800 m a.s.l.). The high variability of the snow cover and
265 moderately low temperatures mean high thermal variability on the ground, melt processes and
266 surface water flow during the winter period. Slab avalanches are very frequent, around 10 per
267 year over the study period. They have no geomorphological effects but lead to snow over-
268 accumulation and a late melt in the lower parts of the debris talus and cones with important
269 implications for the ground thermal regime.
270 Table 1
271 The freeze and frost shattering affects the walls, which remained free of snow in all years,
272 whereas on the debris cones this was minimal due to the low altitude and snow protection.
273 Thus, cryogenic processes have a very modest presence in the cones analyzed.
274 - **Scree accumulation and processes**. Large landslides or rockfalls have not been detected on
275 the cones studied since 1946, only debris flow events reworking the existent features. On the
276 SE face a photograph taken by H. Obermaier in 1914 shows the slopes occupied by blocks
277 and debris while the plain is free of them, but by 1946 debris covered 60.5% of the surface of

278 the plain and slopes. Ten years later a large rockfall of 46,000 m^2 covered half the plain,
279 showing sliding on the snow. A photograph taken by E. Hernández-Pacheco (1956) shows
280 very fresh deposits. Three large rock falls were detected between 1940 and 2005 (two
281 between 1940 and 1956, and one in 2004-2005) with a minimum recurrence of 0.04 events
282 per year. The last rockfall was a small one of 1,000 m^2 between 2003 and 2005 when the area
283 occupied by debris reached 97% of the intramoraine plain (Figure 4). Accumulation rates on
284 the wall base show a fall in activity in the walls since the mid-twentieth century.
285 Only debris flow features and a small rock fall were detected on the cones studied between
286 1946 and 1981. The debris flow events continued over the following ten years, but there were
287 only two debris flows in C-2 and C-1 over the nine years of observations, and there have been
288 a minimum of 14 events recorded in the last 70 years (0.19 events per year). Observation of
289 snow avalanches over the last 10 years shows there are very common successive annual
290 events, predominantly slab avalanches and wet dirty snow avalanches in spring. They reach
291 the proximal and middle parts every year, though snow avalanches can also carry boulders
292 and fine sediments to distal parts.
293 Figure 4
294 **Volumetric changes on debris cones**
295 Annual volumetric changes (Figure 5) detected by the TLS survey on debris cones 1 and 2
296 (Table 2) show considerable variability over the five years analyzed (Table 2) and net
297 differences in sediment redistribution on the cones.
298 Table 2
299 - **Cone A** presents a steep slope (33º-35º) and straight-line morphology (Figure 6A). Annual
300 changes in volume show alternation between loss and increase. Increased volume coincides
301 with years of stable snow cover and volume loss with unstable snow cover. Total volume
302 change shows a moderate increase in sediments, 121,22 m^3 over five years. The behavior by

parts shows clear differences (Figure 5, Table 2). In the middle and proximal parts the accumulation is greater than in the distal one. In the proximal part the accumulations overlap with the deepest incisions linked to the debris flow channel where incisions of around a meter take place. The proximal part is fed by rockfalls and snow avalanches and shows moderate sediment input. The middle part is where the accumulation is greater, showing thickening of around 34%, which is 9 times greater than in the distal part. Longitudinal structures are interpreted as displacement by debris lobes and though the coarsest materials are transported mainly by debris flow, the debris lobes are predominant. The middle and proximal parts contain 71% of the areas with thickening. In 2013-2014 a debris flow event brought about a moderate channel incision (25-50 cm). The distal part shows the highest volume loss rates, mainly in the central and eastern parts. The materials go down towards two dolines, partially filled by boulders and fine sediments.

Figure 5.

As a whole, the volume loss rates for the entire cone are between 0.5 and 25 cm^3, the highest appearing in the central and eastern parts where the lobes and debris flow indicate greater morphogenetic activity (Figure 3, C and D). The longitudinal structures point to the redistribution of dominant processes from the proximal part, where material accumulates by rock fall and snow avalanches with accumulation rates of 2,74 mm a^{-1} towards the distal part moved by debris lobes on 86% of the surface and by debris flow on the remaining 14%. Changes detected in the debris lobes are around 0-25 cm thick in 2010-2011, 2011-2012 and 2013-2014. The largest thicknesses in the longitudinal structures are detected in 2010-2011, when changes of less than 0.50 cm are dominant, though changes between 0.50-100 cm are common (Figure 5). Volume increase is estimated as a minimum sediment input of 24 m^3 a^{-1}.

Figure 6

- **Cone B** possesses a concave-convex profile with a slope of 33º-35º becoming more moderate at the distal part (29º) (Figure 6A). The data show accumulation between 2009 and

2011 and volume loss in 2012-2013 without a direct link to the snow cover changes (Figure 5). The total volume change shows an increase in sediments of 4,642 m^3 over five years and negative values are only found in 2012-2013 (2C). The proximal part shows an increase of >50-100 cm while the main changes were detected in the middle part, where volume loss is dominant (Figure 6). In the proximal part, deep incisions in the debris flow channel show changes in net accumulation or erosion (50->100 cm) together with boulder increase. In the middle part thickening is 18 times greater than in the distal part. The middle and proximal parts contain 84% of the areas with thickening. (Table 2). The five-year trend showed a net accumulation of 1,588.41 m^3 linked to rock fall and snow avalanches with an accumulation rate of 35.5 mm a^{-1}.

The negative values, corresponding to volume loss, are concentrated in the debris flow areas with changes of around 25-100 cm a^{-1}. Thickening is dominant, the data showing between 0,2 and 50 cm with the largest changes appearing in the debris flow channels, which were infilled by more than 1 meter of debris between 2009-2010 and 2011-2012. Measurements of the boulder fabric indicate (Figure 7) dominance of sliding fabric as a result of rockfall over snow cover in spite of the transversal orientation of 20% of the boulders. In the middle part longitudinal orientations and sliding fabric are dominant, linked to the presence of debris lobes. The rolling fabric boulders from rockfalls or snow avalanches reach the middle part, where there are longitudinal and transversal structures and accumulation rates have been estimated at 36.88 mm $a^{-1.}$ The transversal structures show undulations of around 50->100 cm in areas of boulder accumulation with dominance of sliding fabric (Figure 7). This organization coincides with mass movements such as slope slide and shallow slide-earthflow, indicating a change of process in the distal part. The presence of slides may be attributed to slopewash and settling, helped by water availability and sediment output.

Figure 7.

Changes in total cone volume were homogeneous in 2009-2010, 2010-2011 and 2013-2014, with an abrupt change in 2012-2013 when positive deformations doubled, and in 2012-2013 when the value was moderately negative at -663 m^3. Cone B, in the debris flow area, has volume loss rates of around 50-100 cm (Figure 3 E). During the five years volumes increased and, although variability was high, a minimum input sediment of 928 m^3 a^{-1} is estimated, equivalent to 26.2 mm a^{-1}.

From top to bottom Cone B shows different processes (Figure 8: at the top rockfall and debris flow are dominant, in the middle creep develops debris lobes with longitudinal structures and in the distal part slow slide earthflow, slope wash and setting deforming the profile and generating transversal structures. Figure 7C shows the dynamic differences between the two cones. Cone A loses volume in the proximal area and accumulates moderately in the distal, whereas Cone B presents net accumulation in the proximal area, loss of volume in the middle and net accumulation in the distal.

Figure 8

4. Discussion

The processes involved in the debris dynamic imply feeding on the talus and the displacement of clasts over the talus. At first the feed of clasts came from the walls and the vertical rock channel crossing the walls and the debris accumulations where a wide range of processes and changes have been detected from the proximal to the distal parts. Rapp (1960) defined four types of processes: subsidence, talus creep, individual rolling, and small slides, and later debris shift and debris flow were included as determinant processes (Gardner, 1968,1983; Van Steijn,1988 Luckmann, 2013b), all of them transferring the sediments and reworking the morphology of the cones by increasing or reducing their volume by sectors. Processes referred to as "talus creep" by A. Rapp (1960) are related to the presence of ice on the ground, and Van Steijn (1988) referred to "debris shift" as a wide variety of processes.

379 The recognition of different types of slope processes as individual or related events (Figure 8)
380 helps to provide an understanding of debris transfer mechanisms in slopes and debris cones
381 (Luckmann, 1988, 2013b; Van Steijn, 2002). In the Rocky Mountains, Moore et al. (2009)
382 proposed that the segregation of ice is not a determinant agent, so mechanisms such as
383 topographic or tectonic stress and also paraglacial dynamics must be taken into account. Hales
384 and Roering (2005) in the New Zealand Alps point to the local relief, the erosion linked to
385 faulting or jointing and the slope dip as the most significant factors. Most of the studies on the
386 dynamics of debris cones are related to the presence of permafrost or seasonal ice, but in the
387 temperate high mountain the large talus and debris cones are located at low altitude in
388 environments without seasonal ice and with a winter snow cover that protects the ground from
389 frost. The moderate freezing index and low annual freeze/thaw cycles (20-50, Pisabarro et al.
390 2017) favor physical weathering on the walls, located for three months per year at the lower
391 limit of the frost cracking window (-3 to -5ºC), where temperatures are between -6 and -3ºC,
392 the range most sensitive to frost cracking in limestone (Matsuoka, 2001). At present, the low
393 freezing index means that these processes are not determinant in the accumulation of clasts at
394 the foot of the walls (Pisabarro et al. 2017). As in the Rocky Mountains (Moore et al., 2009),
395 in the Picos de Europa the processes of rock mass strength coinciding with a tectonic line, a
396 fracture and thrust, determine variations in rockfall production. Measurements have been
397 taken on debris lobes on the north face of Peña Vieja at 2437 m a.s.l. and Tesorero peak at
398 2320 m a.s.l. The displacement estimated on Peña Vieja was 0.23/0.31 cm a^{-1} and on Tesorero
399 slope between 1.88 and 1.41 cm a-1 (Brosche, 1994), both understood as gelifluction lobes
400 with frost action though located above the cones studied and both north oriented.
401 On the eastern side changes have been frequent at the foot of the 500 m high walls on a plain
402 enclosed by a moraine (Figure 4) attributed to the Dryas (Serrano et al. 2012, 2017), where
403 the scree feed is linked to a large debris fall and debris flow, and climate-determined

variations can take place in scree production. The study area would have been entirely deglaciated at the end of the Younger Dryas around 11 ka (Serrano et al. 2013) and thrust emplacement and paraglacial strength may be the determinant factors in the effectiveness of rock fall processes but also periglacial ones on walls during cold stadia.

The measurements using TLS indicated moderate annual changes of between 2 and 50 cm, mainly by the redistribution of fall material by debris flows and snow avalanches, but not by feed from the walls.

The organization of debris cones is characterized by the dominance of accumulation in the proximal part with intense erosion processes caused by debris flow events and significant annual changes. The low intensity-high frequency nivation processes shifts clasts downslope. Rockfall, debris flow, and snow avalanches bring fine and coarse sediments to the middle parts and generating longitudinal lobes and boulder alignment. The debris cone can therefore be considered as subsystem II in the sediment cascade concept, in which the sediments are stored and reworked (Davies and Korup, 2010).

On the debris cones can be distinguished minor morphogenetic subsystems because changes in processes, structures and accumulation rates. Both cones show the same dynamic by parts (proximal, middle and distal, Figures 5 and 6). The most active processes are located in the proximal (accumulative) and the distal parts. The behavior of the two cones was the opposite of one another in three of the five years observed (Figure 5 and 6, Table 2). Cone B was more active and unstable with higher accumulation rates and annual variability affecting 8.7% of its surface, while only 0.54% of Cone A was affected by annual changes. There are no visible trends over the five years studied, although in 2012-2013 both cones lost volume and in 2013-2014 both increased in volume. Sediment transfer inside the cones was responsible for the cone profile and brought on linked processes between the proximal and middle parts and the middle and distal ones.

- **The proximal part** shows alternate thinning and thickening. Rock fall and snow avalanches bring fine and coarse sediments with boulders that reach the middle part of the cones. Van Steijn (2002) showed that the cones correspond to slow evolution, with massive deposits characterized by century recurrences and highly episodic processes such as rockfall, debris flows, and snow avalanching, in a high magnitude-low frequency system.

The transversal orientations of the boulders indicate the origin of boulders from snow avalanches in the middle parts. Dirty snow avalanches only reach the distal parts in extraordinary events.

Debris flows are the most efficient process in modifying the upper part, but to a greater extent also the middle and distal parts. This has been well studied often in association with the melt of the active layer in permafrost environments, but also related to snow avalanches and swift snow melt or intense precipitations (Decaulne and Saemundsson, 2006). The abundance of fine sediments in the proximal part is critical in facilitating debris flow in the high parts of cones (Hinchliffe et al., 1998). In La Vueltona, snow patches persist until July-August saturating the debris deposits in the apex. Intense precipitation and melt from snow patches support the rapid water availability on partially saturated deposits and the genesis of debris flow along pre-existing channels. The known debris flows during the last ten years are all linked to intense rainfall.

The minimum recurrence of debris flows estimated in the area studied is 0.19 events per year for the last seventy years, and in the debris cones a minimum recurrence of 0.2 events per year over the last ten years. In similar environments estimated recurrences are of 0.025 events per year in Swedish Lapland (Rapp and Nyberg, 1981), 0.15 events per year in the Rocky Mountains (Gardner, 1979), between 0.5 and 2.5 events per year in the Alps (Blijenberg, 1998) and 0.2-0.5 events per year in Iceland (Decaulne et al. 2005). Our data are in accordance with wet temperate environments in the Rocky Mountains and Iceland. The high

454 frequency of debris flow favor sediment transfer more than do snow avalanches in wet
455 environments with thick snow cover (Van Steijn, 2002).
456 - **The middle part** shows important changes of around 0.75-100 cm in Cone B. Scattered
457 large blocks and rolling fabric of the boulders point to the arrival of clasts by snow avalanches
458 and rockfalls, consistent with feeding by the denominated snow avalanche boulder tongue
459 transition deposits (Jomelli and Francou, 2000) rather than by rockfall. But in both cones the
460 dominant landforms in the middle part are the metric to decametric debris lobes together with
461 the debris flow channels. Creep is the main process in the redistribution of materials on the
462 debris cone surface, showing a longitudinal structure by thinning and thickening along the
463 slope. In the absence of frost, creep works through saturation by snow melt waters, as has
464 been established in other high mountains (Pérez, 1985, 1988). The dynamic of the debris
465 lobes is related to water availability by snow melt under the snow cover from March to July.
466 Accumulation of debris is moderate in Cone A (1.4 mm a^{-1}) and high in Cone B, which has
467 accumulations of 36.88 mm a^{-1}.
468 - **The distal part** is characterized by the accumulation of large boulders and digitate tongues
469 of debris flows. The distal part undergoes smaller volume changes and accumulation rates,
470 loss of volume, erosion and sediment output (figure 7) and the flow structures change
471 completely with transversal structures dominant. Debris lobes are less common and the open
472 work by slopewashing is unfavorable to their presence. Nevertheless, the transversal
473 structures are not consistent with the gradient of the slope. These structures have not
474 previously been analyzed in high mountain talus and cones, though Rapp (1960) pointed to
475 the presence of subsidence in the debris cones. The reactivation of distal slides and slow slide-
476 earth flow may be correlated to the presence of undetected seasonal ice in the area or to
477 washing and oversaturation causing local subsidence and slide processes in small depressions
478 (Figure 7). These distal movements may be consistent with gravitational and meltwater-

induced processes (creeping, sliding) taking place in alpine debris cones, predominantly at the lower end of the talus slopes, where concave-up slope profiles are sometimes generated (Kellerer-Pirklbauer and Kaufmann, 2007). Although these authors relate the processes to the presence of mountain permafrost, the supply of snowmelt water to the lower part of the cones may have the same consequences as those brought by the melting of frozen bodies. Whatever the case, in warm and wet mountains deformations by flow of possible frozen bodies must be discarded.

Accumulation rates point to changing values between the proximal part, where values are high in both cases, the middle part, with the higher values in Cone B and moderate ones in Cone A, and the distal one, where accumulation rates are less than 10 mm (Table 2). The accumulation and erosion rates are lower when the time interval is longer (Sadler, 1981; Gardner et al. 1987; Sanders, 2012) since the initial rate of scree deposition may be higher. As the debris accumulation may have begun 11 ka ago, erosion rates could have been higher than those of the present day. The estimated mean accumulation rates of between 1.6 and 26.21 mm a^{-1} are very different indicating a highly dynamic Cone B and a less active Cone A. Both are located at similar altitudes with similar climate conditions and environment. The very different rates show the importance of topography, tectonic setting, glacial erosion and nival processes rather than climate determined processes. As we previously pointed out (Sanders, 2012), under certain geological circumstances talus accumulation can develop in comparatively low topographic locations under warm climatic conditions. Accumulation rates are consistent with measurements in the temperate high mountain of the Rocky Mountains and the Alps, where accumulation rates have been estimated between 1 and 60 mm a^{-1} (Gardner, 1983; Luckmann, 1988; 2013b; Wieczorek et al., 2008; Sanders, 2012; Krautblater and Dickau, 2017;).

503 The present-day low accumulation rates in formerly glaciated areas have led to the suggestion
504 of a paraglacial origin linked to rapid accumulations when accelerated rockwall failures and
505 exposure to atmospheric conditions coincide following glacier recession (Ballantyne, 2002),
506 mainly reflecting a paraglacial environment in a wet mountain climate.

507 **5. Conclusion**

508 The TLS survey and geomorphological analysis applied on two debris cones in the humid
509 temperate mountains has facilitated data of annual topographic changes and transfer of
510 sediments from the walls (subsystem I) to the cones (Subsystem II) in the cascade sediments
511 concept. The combination of TLS and detailed scale geomorphological surveys has facilitated
512 the knowledge of the processes involved in the talus dynamic and the rates of change on the
513 slopes. The application of TLS has been effective in detecting the way debris and transversal
514 flows function, and in monitoring annual topographic changes, but if we wish to establish
515 trends more annual surveys must be conducted.

516 The mean accumulation rates of the talus are high, from 24.2 and 80.7 m^3 a^{-1}, but not too
517 much higher than mean accumulation rates of other scree accumulations in the temperate high
518 mountain. Changes in topography are around 50-100 cm a^{-1} at specific points, but active
519 debris lobes accumulate between 1.6-26.2 mm a^{-1} at altitudes between 1900 and 2200 m.

520 The air and ground temperature data show processes unrelated to frost on talus and cones,
521 where debris flows, snow avalanches, creep, and slides are the main processes involved in the
522 sediment transfer of subsystem II. Climatic conditions and geomorphic indicators as the
523 accumulation rates and processes permit us to propose a paraglacial environment linked to the
524 morphotectonic setting and a wet climate.

525 There is an equilibrium between accumulation and transfer of sediments in Cone A, whereas
526 in Cone B accumulation processes are dominant in the upper part and sediment transfer in the
527 distal one. the most important processes in the morphological evolution of debris cones in the

areas studied are four. Debris flow, which affects the proximal parts and reworks the medium and distal ones. Snow avalanches, which bring materials to the intermediate parts and only exceptionally to the lower ones. Creep, associated with snow melt and manifested through debris lobes. Finally, creep and slide earthflow linked to subsidence generate transversal structures in the low areas.

The debris cone dynamic is defined by the changeover from high intensity-low frequency processes (debris flow, avalanches) in the proximal part, to high frequency-low intensity ones (creep, shift, solifluction) in the middle and distal part, always crossed by downward debris flow.

Acknowledgments

This research was supported by the I+D+I CGL2015-68144-R (Ministerio de Economía y Competitividad) project (FEDER) and the Government of Extremadura (file number GR10071 FEDER).

References

Ballantyne, C.K., 2002. Paraglacial geomorphology. Quaternary Science Reviews 21, (18-19), 1935-2017.

Bauer, A., Paar, G., Kaufmann, V., 2003. Terrestrial laser scanning for rock glacier monitoring, in: M. Philips, S.M. Springth and L.U. Arenson (eds.), Proceedings of the 8ª International Conference on Permafrost. IPA, Zurich, pp. 55-60.

Becht, M., Haas, F., Heckmann, T., Wichmann, V., 2005. Investigating sediment cascades using field measurements and spatial modelling, In: Sediment Budgets (Proceedings of symposium S1, Seventh IAHS Scientific Assembly). IAHS Publ. 291, pp. 2006-2013.

Blijenberg, H.M., 1998. Application of physical modelling of debris flow triggering to field conditions: limitations posed by boundary conditions. Engineering Geology 91, 25-33.

552 Brosche, K.U., 1994. Ergbenisse von Abstragungsmessungen an periglazialen Solifluktions
553 schuttdecken in vier Hochgebirgen der Iberischen Halbinsel (the Picos de Europa, Peña
554 Prieta, Sierra de Urbión und Sierra Nevada). E&G Quaternary Science Journal 44, 28-55.
555 Caine, N. ,1969. A model for alpine talus slope development by slush avalanching. Journal of
556 Geology 77 (1), 92-100.
557 Caine, N., 1974. The geomorphic processes of the alpine environment, In: J. D. Ives, R. G.
558 Barry (eds.), Arctic and Alpine Environments. Methuen, London, pp.721-748.
559 Castañón, J.C., Frochoso, M., 1994. El periglaciarismo de la Cordillera Cantábrica, In:
560 Gómez Ortiz, M. Simón Torres, F. and Salvador Franch, F.(eds.), Periglaciarismo en la
561 Península Ibérica, Canarias y Baleares. Estudios significativos. SEG, Granada, pp.75-91.
562 Castañón, J.C., Frochoso, M., 1998. La alta montaña cantábrica: condiciones térmicas y
563 morfodinámica en los Picos de Europa, In: A. Gómez Ortiz, M. Salvador Franch, F.
564 Schulte and L. García-Navarro, A (eds), Procesos biofísicos actuales en medios fríos.
565 Universidad de Barcelona, Barcelona, pp. 113-132.
566 Davies, T.R.H., Korup, O., 2010. Sediment cascades in active landscapes, In: T. Burt, J.R.
567 Allison, (eds.), Sediment cascades: an integrated approach. Wiley-Blackwell, Oxford, pp.
568 89-116.
569 Decaulne, A., Sæmundsson, O., 2006. Geomorphic evidence for present-day snow-avalanche
570 and debris-flow impact in the Icelandic Westfjords. Geomorphology 80, 80–93.
571 Decaulne A., Sæmundsson, O., 2010. Distribution and frequency of snow-avalanche debris
572 transfer in the distal part of colluvial cones in Central North Iceland. Geogrphiska Annaler
573 92 A, 177–187.
574 Decaulne, A., Saemundsson, Th., Petursson, O., 2005. Debris flows triggered by rapid
575 snowmelt in the Gleidarhjalli area, northwestern Iceland. Geografiska Annaler 87A, 487-
576 500.

577 Delaloyé, R., Reynard, E., Lambiel, C., Marescot, L., Monnet, R., 2003. Thermal anomaly in
578 a cold scree slope, Creux du Van, Switzerland, In: M. Philips, S.M. Springth, L.U. Arenson
579 (eds.), Proceedings of the 8ª International Conference on Permafrost. IPA, Zurich, pp. 175-
580 180.
581 De Haas, T., Kleinhans, M. G., Carbonneau, P. E., Rubensdotter, L., Hauber E., 2015. Surface
582 morphology of fans in the high-Arctic periglacial environment of Svalbard: controls and
583 processes. Earth-Science Reviews 146, 163–182.
584 Farias, P., 1982. La estructura del sector central de los Picos de Europa. Trabajos de Geología
585 12, 63-72.
586 Fengqing, J., Yanwei, Z., 2011. Freezing and thawing index, in: V.P. Singh, P. Singh, U.
587 Haritashya, (eds.), Encyclopedia of snow, ice and glaciers. Springer, Dordrecht, pp. 301.
588 Fey, C., Wichmann, V., 2017. Long-range terrestrial laser scanning for geomorphological
589 change detection in alpine terrain-handling uncertainties. Earth Surface Processes and
590 Landforms 42, 789-802.
591 Francou, B., 1983. Géodynamique des dépots de pied de paroi dans l´etage périglacial. Revue
592 de Géologie Dinamique et Geographie Physique 24 (5), 411-424.
593 Francou, B., 1988. L'Eboulisation en Haute Montagne. Editec. Grenoble.
594 Francou, B., 1991. Pentes, granulométrie et mobilité le long d'un talus d'éboulis en milieu
595 alpin. Permafrost and Periglacial Processes 2, 175-186.
596 French, H.M., 2007. The periglacial environment. Wiley and Sons, Chichester.
597 Gardner, J.S., 1968. Debris slope form and processes in the Lake Louise District: a high
598 mountain area. Department of Geography, McGill University, Montréal.
599 Gardner, J.S., 1979. The movement of material on debris slopes in the Canadian Rocky
600 Mountains. Zeitschrift fur Géomorphologie 23, 45-67.

601 Gardner, J.S., 1983. Accretion rates on some debris slopes in the Mt. Rae Area, Canadian
602 Rocky Mountains. Earth Surface Processes and Landforms 8 347-355.
603 Gardner, J.S., 1983. Observations on erosion by wet snow avalanches, Mount Rae area,
604 Alberta, Canada. Arctic and Alpine Research 15, 271-274.
605 Gigli, G., Morelli, S., Fornera, S., Casagli, N., 2014. Terrestrial laser scanner and
606 geomechanical surveys for the rapid evaluation of rock fall susceptibility scenarios.
607 Landslides 11(1), 1-14.
608 González-Trueba, J.J. , 2007a. El paisaje natural del Macizo Central de los Picos de Europa.
609 CIMA, Consejería de Medio Ambiente, Santander.
610 González-Trueba, J.J., 2007b. Geomorfología del Macizo Central del Parque Nacional de
611 Picos de Europa. OAPN-Ministerio de Medio Ambiente, Madrid.
612 González-Trueba, J.J., Serrano, E., 2010. Geomorfología del Macizo Oriental del Parque
613 Nacional de Picos de Europa. OAPN-Ministerio de Medio Ambiente, Madrid.
614 Götz, J., Otto, J.C., Schrott, L., 2013. Postglacial sediment storage and rockwall retreat in a
615 semi-closed inner-alpine basin (Gradenmoss, Hohe Tauern, Austria). Geografia Fisica e
616 Dinamica Quaternaria 36 (1), 63-80.
617 Goudie, A., 1981. Geomorphological Techniques. Allen & Unwin, London.
618 Hales, T. C., Roering, J. J., 2005. Climate-controlled variations in scree production, Southern
619 Alps, New Zealand. Geology 33(9), 701-704.
620 Herz, T., King, L., Gubler, H., 2003. Microlimate whithin coarse debris of talus slopes in the
621 alpine periglacial belt and its effect on permafrost, in: M. Philips, S.M. Springth and L.U.
622 Arenson (eds.), Proceedings of the 8ª International Conference on Permafrost. IPA, Zurich,
623 pp. 383-388.

624 Hinchliffe, S., Ballantyne, C.K., Walden J., 1998. The structure and sedimentology of relict
625 talus, Trotternish, northern Skye, Scotland. Earth Surface Processes and Landforms 23,
626 545-560.
627 Jomelli, V., Francou, B., 2000. Comparing characteristics of rockfall talus and snow
628 avalanche landforms in an alpine environment using a new methodological approach.
629 Geomorphology 35, 181-192.
630 Kellerer-Pirklbauer, A., Kaufmann, V., 2007. Paraglacial talus slope instability in recently
631 deglaciated cirques (Schober Group, Austria). Grazer Schriften der Geographie und
632 Raumforschung 43, 121-130.
633 Kirkby, M., Statham, I., 1975. Surface stone movement and scree formation. Journal of
634 Geology 83(3), 349-362.
635 Kotarba, A., Kaszowski, L., Krzemien, K., 1987. High mountain denudational system of the
636 Polish Tatra Mountains. Polish Academy of Science, Kracow.
637 Kotarba, A., Klapa, M., Midriak, R., Petras, J., Skroda, J., 1979. Field experiments on high
638 mountain slopes of the Tatra Mts. Studia Geomorphologica Carpatho-Balcanica 13, 132-
639 148.
640 Krautblatter, M., Dikau, R., 2007. Towards a uniform concept for the comparison and
641 extrapolation of rockwall retreat and rockfall supply. Geografiska Annaler 89A, 21-40.
642 Luckman, B.H., 1976. Rockfalls and rockfall inventory data: some observations from Surprise
643 Valley, Jasper National Park, Canada. Earth Surface Processes and Landforms 1, 287-298.
644 Luckman, B.H., 1988. Debris accumulation patterns on talus slopes in Surprise Valley,
645 Alberta. Géographie Physique et Quaternaire 42 (3), 247-278.
646 Luckman, B.H., 2013a. Processes, transport, deposition and landforms: rockfall, in: J.
647 Shroder, R.A. Marston, M. Stoffel (eds.), Treatise on Geomorphology, vol. 7, Mountain
648 and Hillslope Geomorphology. Academic Press, San Diego, pp. 174-182.

649 Luckman, B.H., 2013b. Talus Slopes, in: S.A. Elias (ed.), The Encyclopedia of Quaternary
650 Science. Elsevier, Amsterdam, pp. 566-573.
651 Marquínez, J., 1989. Síntesis cartográfica de la región del Cuera y los Picos de Europa.
652 Trabajos de Geología 18, 137-144.
653 Marquínez, J., 1992. Tectónica y relieve en la Cornisa Cantábrica, in: A. Cearreta, F.M.
654 Ugarte (eds.), The late Quaternary in the western Pyrenean region. Universidad del País
655 Vasco, Vitoria, pp. 143-160.
656 Moore, J.R., Sanders, J.W., Dietrich, W.E., Glaser, S.D., 2009. Influence of rock mass
657 strength on the erosion rate of alpine cliffs. Earth Surface Processes and Landforms 34,
658 1339-1352.
659 Otto, J.C., Schrott, L., Jaboyedoff, M., Dikau, R. 2009. Quantifying sediment storage in a
660 high Alpine valley (Turtmanntal, Switzerland). Earth Surface Processes and Landforms 34
661 (13), 1726-1742.
662 Pérez, F.L., 1988. The movement of debris on a high Andean talus. Zeitschrift für
663 Geomorphologie 32, 77-99.
664 Pérez, F.L., 1993. Talus movement in the high equatorial Andes: a synthesis of ten years of
665 data. Permafrost and Periglacial Processes 4, 199-215.
666 Pérez, F.L., 1998. Talus fabric, clast morphology, and botanical indicators of slope processes
667 on the Chaos Crags (California Cascades), USA. Géographie Physique et Quaternaire 52
668 (1), 1- 22.
669 Pisabarro, A., Pellitero, R., Serrano, E., Gómez-Lende, M., González-Trueba, J.J., 2017.
670 Ground temperatures, landforms and processes in an Atlantic mountain. Cantabrian
671 Mountains (Northern Spain). Catena 149, 623-636

672 Phillips, M., Mutter, E.Z., Kern-Luetschg, M., Lehning, M., 2009. Rapid degradation of
673 ground ice in a ventilated talus slope: Flüela Pass, Swiss Alps. Permafrost and Periglacial
674 Processes 20, 1-14.
675 Rapp, A., 1960. Recent development of mountain slopes in Karkevagge and surroundings,
676 northern Scandinavia. Geografiska Annaler 42, 65-200.
677 Rapp, A., Fairbridge, R.W., 1968. Talus fan or cone, in: R.W. Fairbridge (ed.), Encyclopaedia
678 of Geomorphology. Van Nostrand Reinhold, New York. pp. 1106-1109.
679 Rapp, A., Nyberg, R., 1981. Alpine debris flows in northern Scandinavia: morphology and
680 dating by lichenometry. Geografiska Annaler 63A, 183-196.
681 Rosser, N.J., Petley, D.N., Lim, M., Dunning, S.A., Allison, R.J., 2005. Terrestrial laser
682 scanning for monitoring the process of hard rock coastal cliff erosion. Quarterly Journal of
683 Engineering Geology and Hydrogeology 38, 363–376.
684 Sadler, P.M., 1981. Sediment accumulation rates and the completeness of stratigraphic
685 sections. Journal of Geology 89, 569-584.
686 Sanders, D., Ostermann, M., Kramers, J., 2009. Quaternary carbonate-rocky talus slope
687 successions (Eastern Alps, Austria): sedimentary facies and facies architecture. Facies 55,
688 345-373.
689 Sanders, D., 2012. Talus accumulation in detachment scars of Late Holocene rock avalanches,
690 Eastern Alps (Austria): rates and implications. Géologie Alpine 9, 82-99.
691 Sanjosé, J.J., Berenguer, F., Atkinson, A.D.J., De Matías, J., Serrano, E., Gómez-Ortiz, A.,
692 González-García, M., Rico, I., 2014. Geomatics techniques applied to glaciers, rock
693 glaciers and ice-patches in Spain (1991-2012). Geografiska Annaler 96A, 307-321.
694 Scapozza, C., Lambiel, C., Baron, L., Marescot, L., Reynard, L., 2011. Internal structure and
695 permafrost distribution in two alpine periglacial talus slopes, Valais, Swiss Alps.
696 Geomorphology 132, 208-221.

Schrott, L., Adams, T., 2002. Quantifying sediment storage and Holocene denudation in an Alpine basin, Dolomites, Italy. Zeitschrift für Geomorphologie 128, 129-145.

Schrott, L., Hufschmidt, G., Hankammer, M., Hoffmann, T., Dikau, R., 2003. Spatial distribution of sediment storage types and quantification of valley fill deposits in an Alpine basin, Reintal, Bavarian Alps, Germany. Geomorphology 55, 45-63.

Selby, M.J., 1983. Hillslope, materials and processes. Oxford University Press, Oxford.

Serrano, E., González-Trueba, J.J., 2004. Morfodinámica periglaciar en el grupo Peña Vieja (Macizo Central de los Picos de Europa -Cantabria-). Cuaternario y Geomorfología 18, 73-88.

Serrano, E., González-Trueba, J.J., Sanjosé, J.J., Del Río, L.M., 2011. Ice patch origin, evolution and dynamics in a temperate high mountain environment: the Jou Negro, Picos de Europa (NW Spain). Geografiska Annaler 93, 57-70.

Serrano, E., González-Trueba, J.J., González-García, M., 2012. Mountain glaciation and paleoclimate reconstruction in the Picos de Europa (Iberian Peninsula, SW Europe). Quaternary Research 78, 303-314.

Serrano, E., González-Trueba, J.J., Pellitero, R., González-García, M., Gómez- Lende, M., 2013. Quaternary glacial evolution in the Central Cantabrian Mountains (Northern Spain). Geomorphology 196, 65-82.

Serrano, E., González-Trueba, J.J., Pellitero, R., Gómez-Lende, M., 2017. Quaternary glacial history of the Cantabrian Mountains of northern Spain: a new synthesis, in: P.D. Hughes and J.C. Woodward (eds.), Quaternary Glaciation in the Mediterranean Mountains. Geological Society, Special Publications, 433, London, pp. 55-85.

Statham, I., 1976. A scree slope rockfall model. Earth Surface and Processes 1, 43-62.

720 Thorn, C.E., Schlyter, P.L., Darmody, R.G., Dixon, J.C., 1999. Statistical relationships
721 between daily and monthly air and shallow-ground temperatures in Kärkevagge, Swedish
722 Lapland. Permafrost and Periglacial Processes 10, 317-330.
723 Van Steijn, H., de Ruig, J. Hoozemans, F., 1988. Morphological and mechanical aspects of
724 debris flows in parts of the French Alps. Zeitschrift für Geomorphologie 32, 143–161.
725 Van Steijn, H., Boelhouwers, J., Harris, S., Hétu, B., 2002. Recent research on the nature,
726 origin and climatic relations of blocky and stratified slope deposits. Progress in Physical
727 Geography 26, 551–575.
728 Wheaton, J.M., Brasington, J., Darby, S.E., Sear, D.A., 2010. Accounting for uncertainty in
729 DEMs from repeat topographic surveys: improved sediment budgets. Earth Surface
730 Processes and Landforms 35, 136–156
731 Vere, D., Mathews, J., 1985. Rock glaciers formation from a lateral moraine at
732 Bukkeholsbreen, Jotunheimen, Norway: a sedimentological approach. Zeitschrift für
733 Geomorphologie 29, 397-415.
734 Wieczorek, G.F., Stock, G.M., Reichenbach, P., Snyder, J.B., Borchers, J.W., Godt, J.W.,
735 2008. Investigation and hazard assessment of the 2003 and 2007 Staircase Falls rock falls,
736 Yosemite National Park, California, USA. Natural Hazards and Earth System Science 8,
737 421-432.
738 **Figures:**
739 Figure 1. Location of the studied area. Red dots indicate the meteorological stations (1, Upper
740 cable car station. 2, Cabaña Verónica station).
741 Figure 2. Up, geomorphological sketch of Peña Vieja Group and surrounding. Number 1 is
742 the debris cone A and number 3 is the debris cone B. Down, detailed geomorphological
743 sketch of debris cones A and B.

744 Figure 3. Debris cones in the Peña Vieja Group, where it is perceptible the relation between
745 wall unevenness and cones development. A. Southwest side, La Vueltona area, 1 and 3 are the
746 studied debris cones A and B. B. Southeast side, Áliva area, debris cones have less
747 development than in the other side. C. Cone B, detail of the surface morphology, debris lobes
748 (L), in the central portion, and debris flow features. D. Debris cone B, note the texture of
749 debris flow channel and fan, and the profile with debris lobe (L). Dfc, debris flow channel.
750 Dfa, debris fan. E, detail of debris fan in debris cone B.
751 Figure 4. Scree infill in the cirque SE of Peña Vieja-Áliva (1946-2014).
752 Figure 5. A. Topographic changes in Cone A (number 1 in Figure 2) and Cone B (number 3 in
753 Figure 2).
754 Figure 6. A, profiles of the cones A and B. B, year on year evolution of volume changes (m^3)
755 and accumulation rates (mm a^{-1}) in debris cones A and B. C, accumulation rates by parts and
756 surface of debris cones A and B.D, vertical changes at different radial distances from the apex
757 (a) Percentiles 25, 50 and 75 for vertical changes experiences by locations in cone A (a) and
758 cone B (b) at different radial distances from the apex.
759 Figure 7. A. Axe L boulder orientations in Cone B by altitude areas. d, slope direction.
760 Representation in percentage. B. Location of represented points in the profile of cone B. C.
761 Slow mass wasting in the distal part of debris cone B. D. Detail of lobes and flow direction
762 where the surface structure visible in TLS diagrams show transversal structures to flow
763 direction.
764 Figure 8. Toposequence of Debris cone B, with representation of processes, landforms and
765 deposits.
766 **Tables:**
767 Table 1. Climatic data of meteorological station and ground thermal records.

768 Table 2. Morphometric data (A), Volume and height changes by years (B), and changes by

769 sections (C) on debris cones of La Vueltona (2009-2014).

*Graphical Abstract

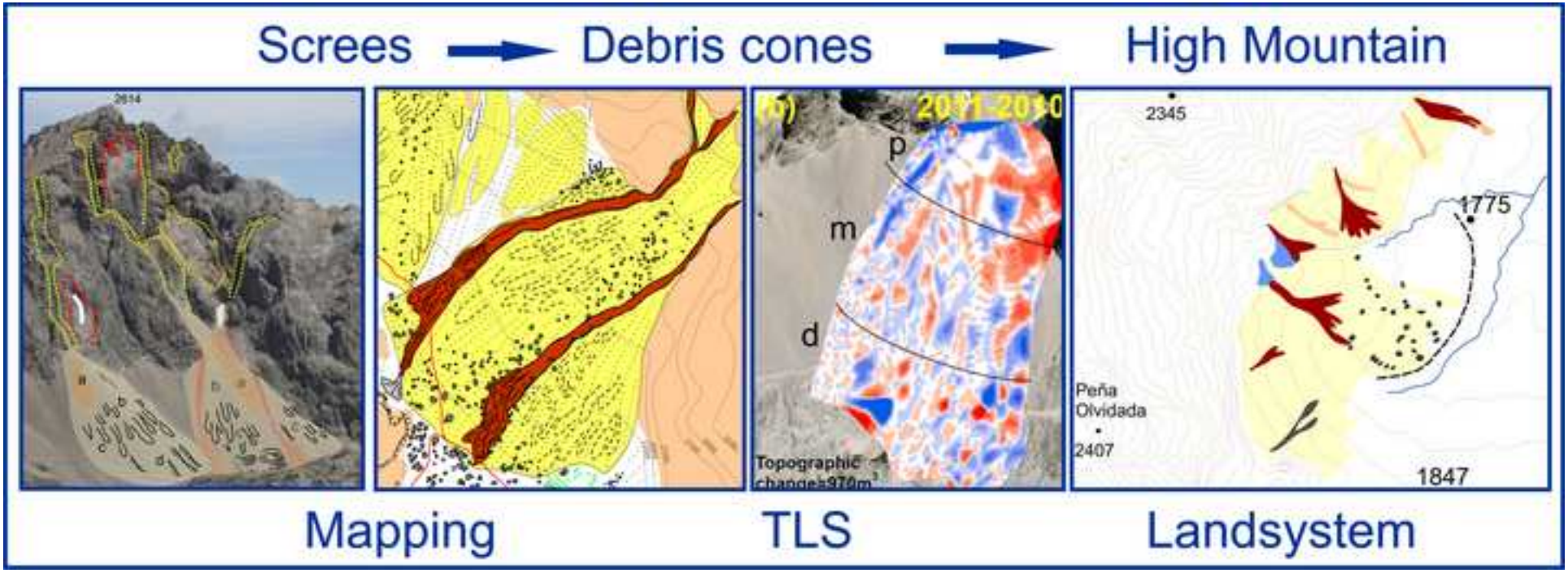

***Highlights (for review : 3 to 5 bullet points (maximum 85 characters including spaces per bullet point)**

- Key elements: A paraglacial environment, tectonic setting and wet mountain climate.

- The debris cones accumulation rates on change between1.6 and 26.2 mm a^{-1}

- Three areas can be differentiate from up to bottom by structures, processes and dynamics.

- The most important changes take place in the proximal and middle parts.

- TLS is a effective technique to monitoring annual volumetric changes and detect debris transfer.

*Revised manuscript with no changes marked (double-spaced and continuously LINE and PAGE numbered)
Click here to view linked References

SURFACE MOVEMENT AND CASCADE PROCESSES ON DEBRIS CONES IN TEMPERATE HIGH MOUNTAIN (PICOS DE EUROPA, NORTHERN SPAIN)

Enrique Serrano[1], José Juan Sanjosé[2], Álvaro Gómez-Gutiérrez[3], Manuel Gómez-Lende[4]

[1]Department of Geography. University of Valladolid, Spain. serranoe@fyl.uva.es
[2] Department of Graphic Expression. University of Extremadura, Polytechnic School, Cáceres Spain. jjblasco@unex.es
[3] Department of Geography. University of Extremadura, Cáceres, Spain. alvgo@unex.es
[4] PANGEA Research Group. University of Valladolid. Spain. manuelglende@hotmail.com

Abstract

Debris talus is a very common landform in the temperate high mountain, so much so that it is the most representative of the periglacial and nival processes. This work studies debris cones in the Picos de Europa, an Atlantic mountain range in the north of the Iberian Peninsula. A detailed geomorphological map was prepared, fieldwork were carried out on the debris cone surface, the ground and air thermal regime was analyzed, and a five-year Terrestrial Laser Scan survey carried out. Annual volume changes on the surface of the debris cones were detected and related to active processes and sediment transfer. Two different behaviors were observed in each cone. Cone A is linear, with equilibrium between accumulation and sediment transfer, while Cone B is concave-convex denoting accumulation processes in the upper part deriving from the greater frequency of snow avalanches. Changes in morphology surpass 50 cm/year with most of the activity taking place in the highest and lowest areas. The presence and action of the ice on the debris slope are moderate or non-existent and freeze-thaw processes are only active on the walls at over 2000 m a.s.l. The main processes on debris cones are debris flow and creep related to snowcover, but sediment transfer on the slopes involves high intensity-low frequency (debris flow, avalanches) and high frequency-low intensity processes (creep, shift, solifluction and wasting).

Key words: Scree slopes, debris cones, slope processes, Terrestrial Laser Scanner, temperate high mountain

1. Introduction.

Debris talus and cones are one of the commonest landforms of temperate mountains and active ones are highly representative of the high mountain with periglacial dynamics. They have been defined as "distinctive accumulations of loose, coarse, usually angular rock debris at the foot of steep bare rock slopes" (Luckmann, 2013). The study of debris talus and cones began by analyzing the topographic position and morphology of talus and cones in cold mountain environments (Rapp, 1960; Rapp and Fairbridge, 1968) before later focusing on genetic processes, their evolution (Caine, 1974; Luckman, 1976, 1988; Kotarba et al, 1979, 1987) and processes involved in sediment and transport on debris talus and cones. Creep processes, snow avalanche relationships, rockfall, debris flows, slush avalanching, gelifluction, gravitational rolling, surface run-off and clast slideover were studied together with deposits, landforms and the internal structures defined by stratified and stocked sediments (Caine, 1969, 1974; Kirkby and Statham, 1975; Luckman, 1976, 1988; Statham, 1976; Kotarba et al., 1979; Gardner, 1979, 1983; Selby, 1983, Francou, 1988, 1991; Hinchliffe et al., 1998; Saas, 2006, Jomelli and Francou, 2000De Haas et al., 2015). A typology of taluses of high mountain environments was established, differentiating between gravitational cones dominated by rockfalls with slopes of around 35º and concave profiles; snow avalanches and boulder tongues with slopes of around 35º and concave to linear profiles; avalanche cones, characterized by slopes of between 27º and 30º segmented in two or three parts with concavity; and debris flow cones, all of them representative of the temperate high mountain (Caine, 1974; Luckman, 1988, 2013b; Selby, 1983, Francou, 1991).

The debris cones and talus dynamic in the high mountain is commonly related to periglacial environments, with higher erosion rates and sediment transfer determined by deglaciation and paraglacial environments (Ballantyne, 2002), but processes related to seasonal frozen ground

and permafrost are also important factors in the dynamic of surface debris cones (Francou, 1988, 1991; Delaloyé et al. 2003; Herz et al. 2003, Scapozza et al., 2011). Investigation on hazard assessment, rockwall retreat and rockfall supply have shown the high complexity linked to previous slides, rock type and environments, without necessarily being cold environments and freeze-related processes (Krautblatter and Dikau, 2007; Wieczorek et al. 2008; Sanders et al. 2009). Previous works have revealed the complexity of processes involved in the dynamic of debris talus and cones, in which there is a broad typology of processes taking part in sediment storage and transfer, all differentiated by environmental conditions, lithology and structure.

As described later, the study area is a glaciokarstic environment without surface drainage in which glacial erosive landforms and rockwalls are linked by debris talus and cones. The debris cones landform system can be divided in two areas, (i) the rock face, the source area for rockwalls, and (ii) the debris cones, a temporary storage where deposits are reworked prior to sediment output. The sediment cascade concept is considered to be the connection between processes and landforms in which the output of one process is the input of another. Depositional landforms work as the temporary storage of sediment output (Davies and Korup, 2010) and so the debris cone is included in the talus slopes system. Previous studies have mainly been focused on the rock wall (subsystem I) and the valley bottom (subsystem III) of the slope sediment cascade, rather than on the talus slope (subsystem II). Sediments are stored and reworked in the debris talus and cones. Denudation and rockwall retreat have been quantified and models established to understand the source area's contribution to sediment flow (e.g. Becht et al. 2005; Klaubatter and Dickau, 2007; Otto et al. 2009; Luckman, 2013a, 2013b). Klaubatter and Dickau (2007) differentiate between stages such as back weathering, filling and depletion of intermediate storage on the rock face and the final rockfall supply onto the talus slopes, but the intermediate sediment storage and processes are often

disregarded (Götz et al. 2013; Schrott and Adams, 2002; Schrott et al., 2003; Otto et al., 2009).

The aim of this work is to analyze the surface changes taking place on two cones by means of geomatic techniques and relate them to surface processes, ground temperatures, temporary storage and transfer process of sediments in temperate high mountains. The research hypothesis was that in the debris cones landform system linked to atlantic high mountain periglacial environments the frozen ground direct the main processes involved in slope sediment cascade.

2. Material and methods

2.1. Study site characteristics.

The Picos de Europa are located in the north of the Cantabrian Mountains (43°10'N/4°50'W) just 20 km from the Cantabrian Sea (Fig. 1). It is a mountain range with abrupt vertical relief and summits of up to 2700 m (Torre Cerrado, 2648 m a.s.l.) and a marked oceanic influence.

Figure 1.

The geological structure constitutes a succession of thrust faults of south vergence divided by faults (Farias, 1982) featuring as a succession of slopes related to north dip and scarped fronts to the south where the main rocky walls are located. Local and regional WNW-ESE faulting breaks up the fronts and forms successive massifs and mountain groups. The predominating rocks are limestone, the “Calizas de Montaña Formation" (Namurien to Westfalian Age), and “Picos de Europa Formation” (Westfalian-Cantabrian Age) with alternating slates, calcareous conglomerate, limestones and turbiditic sandstones of the Stephanian Age (Marquínez, 1989, 1992).

Morphostructural elements together with karstic and glacial features define the relief in the Picos de Europa. Quaternary and Little Ice Age glacial processes have shaped the massif with

106 erosive glaciokarstic landforms and accumulative glacial landforms of different Upper
107 Pleistocene glacial phases (González-Trueba, 2007a, b; Serrano et al. 2012; 2013, 2017).
108 The talus and cones studied are located in a high mountain glacio-karstic landscape with
109 periglacial and nivation processes. Active debris cones and talus are distributed between 1200
110 and 2600 m a.s.l. and are functional above 1900 m a.s.l., where seasonal frozen ground
111 environments develop (González-Trueba, 2007a; Pisabarro et al. 2017).
112 The area studied houses a set of 16 active debris cones (Figure 2) oriented to the N between
113 2350 and 2600 m a.s.l., and S, SE and SW between 1790 and 2230 m a.s.l. . (Serrano and
114 González Trueba, 2004). They are divided in the proximal, medial and distal parts as cones
115 and fans are usually defined (Leeder, 1982; Harvey, 2012). The altitude and proximity to the
116 sea favor a hyperhumid environment characterized by rainfall of around 2500 mm a^{-1} and
117 snow cover duration of around six-seven months per year above 1800 m a.s.l. (González
118 Trueba, 2007a)
119 Figure 2
120 **2.2. Applied techniques**
121 **Geomorphological mapping**
122 This is a key tool in geomorphological system analysis and the basis for understanding
123 landforms, distribution processes and relationships (Smith et al. 2011). From a 1:25.000 scale
124 geomorphological map (Serrano and González-Trueba, 2004; González Trueba, 2007b) a
125 detailed geomorphological survey of debris talus and cones in the Peña Vieja Group was
126 performed. The mapping approach to the debris cones was done by fieldwork with a GIS
127 component. Landforms and processes were digitized on orthophotographs (scale 1:5,000) and
128 a derived digital terrain model (DTM), and during the fieldwork the processes were assessed
129 manually, transferred into a GIS database and initially visualized as a geomorphological map
130 (1:10,000). The landform inventory (Serrano and González-Trueba, 2004; González-Trueba,

2007a, b) was completed by multi-temporal orthophotograph interpretation and the analysis of multidirectional shaded relief and slope grids. The map includes landform type and predominant processes (see fig. 8) of accumulation on debris cones, leading to the establishment of the spatial and altitudinal distribution of processes and the classification between active and relict landforms (Kotarba et al. 1987; Francou, 1988). The use of the sediment cascade concept (Davies and Korup, 2010) helps to organize data of the debris cones systematically, where the distinction can be made between i) sediment input into the cones, ii) sediment redistribution, and iii) output (process-specific and volumetric) (see figure 8).

A diachronic analysis of orthophotos from 1946 to 2014 revealed the large rock fall and debris flow on the SW and NW sides of Peña Vieja Group and its evolution over this 68-year period was mapped.

Coarse texture and fabric

Morphometric, granulometric and orientation analyses were performed by fieldwork in order to know the cone genesis and typology. A slope profile by grids is a very common sampling technique in the study of coarse texture and fabric analysis (Francou, 1983; Pérez, 1998). Four slope profiles were obtained from cone apex to base with 100 data points per grid, and the cone surface was sampled at nine stations along the three profiles. We established a grid of 1 m^2 and the particles inside the grid points were sampled. The area to be sampled was divided into the three areas of the cone, the proximal, middle and distal. In each area three transversally aligned grids were measured. In each grid, boulder-size between 2-24 cm on the L axis, morphometry, lithology and orientation were measured. This technique has been applied widely in the study of slope deposits and debris (Goudie, 1981; Francou, 1983; Vere and Mathews, 1985; Pérez, 1998). Data of boulder size by transect were determined by

measuring the L axis of the 50 largest clasts (> 50 cm L axis) and orientation in the field by compass and clinometer. Only the orientation data were used to establish the L axis layout.

The use of orthophotos facilitates the selection and estimation of areas with upslope imbrication, rolling fabric or sliding fabric of large boulders (over 2 meters) and the classification of coarser deposits such as snow-sliding, rockfall or creep processes, while indicating the different processes involved in the reworking of the debris cones (Kotarba et al., 1987; Francou, 1991; Pérez, 1998; Decaulne and Sæmundsson, 2010).

Thermal analysis

Data were obtained from meteorological stations in the National Park and thermal micro sensors type I-Bottom UTL-Geotest AG data-logger (with centesimal accuracy and 0.05°C error level) buried between 5 and 10 cm depth and emplaced at 1865 m a.s.l. were used to analyze the ground and air thermal regime so that thermal data around the debris cones and thermal differences between walls and deposits could be compared (Thorn et al. 1999; Pisabarro et al. 2017).

Two meteorological stations (OAPN net, Cabaña Verónica hutte -43º10´09´´N/4º50´03´´W, 2309 m a.s.l.-, and Upper station of Cablecar -43º09´08´´N/4º48´18´´W, 1853 m a.s.l.) (Figure 1), located at less than 1,000 metres from both the NW and S of the selected debris cones, were used to analyze air conditions with discontinuous data from 2011-2015. Annual Air Medium Temperatures (AAMT), the number of days with temperatures below 0ºC, the freezing index and frost cycles were calculated (Pisabarro et al. 2017).

Annual Ground Surface Medium Temperatures (AGSMT) were measured by a datalogger located just at the front of the debris cone in an area without vegetation cover that usually presents an important snow cover during the winter. The thermometers monitored ground temperatures between 4 and 6 times a day for an entire year. The data were collected between 2004 and 2007. Representative statistical parameters of temperature tendencies, phases,

freeze/thaw cycles (days with temperatures below and over 0 °C), the freezing index and temporal behaviors were estimated. Frost cycles and freezing index are the most interesting parameters because they permit the comparison of the presence of seasonal ice, depth of seasonal ice, depth of ground ice and snow cover duration related to the intensity, duration and seasonality of ice on the ground (French, 2007; Fengquing and Yanwei, 2011)

Topographic change detection by terrestrial laser scanning (TLS) survey

A TLS survey was carried out in the La Vueltona valley using a TOPCON IS Imaging Station instrument. Terrestrial laser scanning has been widely used to monitor numerous rockwalls and cliffs, glaciers and rock glaciers, to estimate small- to medium-sized volumetric changes and rockfall support (e.g. Bauer et al. 2003; Rosser et al. 2005; Sanjosé et al. 2014; Gigli et al. 2014; Fey and Wichmann, 2017).

The procedure comprised the acquisition of a sector scan from one single scan position located at 2020 m a.s.l, in front of the cones where the shadowing effects are minimal, at between 170 and 610 m from Cone 1 and 330-650 from Cone 2. As the instrument is a Total Station, each scan position was referenced to another two topographic bases to take measurements within the same system of coordinates.

Precise measurements on talus and cones were carried out for the period from 2008 to 2014. Vertical and horizontal accuracies were 1-2 cm and the long-range instrument registers points at a distance of 1000 m with an accuracy of around 2 cm. The TLS was located at an approximate distance of 300 m, 20 points s-1 were registered at distances of less than 150 m while for longer distances 1 point s-1 was captured. These points were used to generate a Digital Elevation Model (DEM) based on a Triangulated Irregular Network (TIN) surface, from which annual spatial variations of volume loss or gain were calculated. As the surface did not have any features above ground (e.g. vegetation or buildings) no filter was applied.

During the fieldwork the survey was performed twice and results compared. The heterogeneity of the clast means that when two surveys are made the points do not all coincide. The points measured are not the same in each survey and the TIN was performed using different DEMs. Therefore, when two surveys are compared the differences between the two scans is greater than 2 cm. As the medium size of boulders on the surface was considered to be ±25 cm, the estimated changes were ±25 cm due to instrument inaccuracy and the generation of the TIN. To calculate the DEM of difference (DoDs), a mesh surface was first generated for each piece of data using the TIN tool implemented within ArcGIS 10.2. These surfaces were then converted to the raster format and subtracted to produce the DoDs. Taking into account the accuracy of the coordinates for each point (≈2 cm), the DoD approach was carried out without any threshold to discriminate noise and geomorphic change. This is a commonly used conservative strategy (Wheaton et al., 2010).

The point density was obtained using a cell size of 3 x 3 m at 500 m distance, though when distances are shorter the cell is denser. Thus, the debris cone distal area has a higher density than the proximal area. The point density is sufficient for this work since the slopes do not undergo significant changes and the differences between the two TINs during the same survey are greater than 25 cm, which coincides with the medium size of boulders. The instrument measures one point every 3-4 seconds for about eight hours to obtain 4000 points per TIN. The model has a point cloud of 8000 points distributed over 16,027 m^2 for Cone A and 15,575 m^2 for Cone B.

3. Results

Processes and environment

The active debris cones are widespread from 1900 m a.s.l. and there is practically no vegetation on them. They vary in height between 170 and 319 m with slopes between 32º and

228 36º and an h/H index that is always low (Serrano and González-Trueba, 2004). Large walls
229 with little talus or cone development are predominant (Figure 3).
230 Figure 3.
231 The detailed geomorphological maps (Figure 2) reveal four dominant surface processes. The
232 main surface processes by area on the debris cones are metric to decametric debris lobes,
233 sometimes configured as block streams (Figure 2B). Debris flow, characterized by depth
234 channels of between 1 and 3 meters linked to a debris fan, is the most energetic sediment
235 transfer process in the cones analyzed. Debris flow are the second most important process by
236 area, with faster and more efficient debris transfer systems between the proximal and distal
237 parts. During the last ten years this process has been detected twice, once in each cone and in
238 different years, 2011 and 2013. Rockfalls generate boulders scattered throughout the talus
239 and cones, although the sliding fabric indicates sliding over a seasonal snow cover and creep
240 as common processes. Slide and creep are two important processes of redistribution of
241 materials on the surface of the cones. They form metric to decametric debris lobes located
242 mainly in areas with steeper slopes and made up of fine and coarse materials. They outline
243 longitudinal clast flows that move faster than the surrounding debris.
244 The debris cones studied form a part of the sediment storage and redistribution as sediment
245 transfer system toward output of the slope system. The proximal part is characterized by small
246 debris flow channels and scattered boulders with finer debris. The boulders are mainly falling
247 and rolling boulders that have come to rest at the edge of the cones, but sliding fabric is also
248 common. In the central part metric-sized debris lobes predominate supporting a homogeneous
249 slope with scattered boulders and depth debris flow channels crossing it, sometimes
250 depositing debris fan. Debris lobes are located mainly in the central and lateral areas where
251 the slope reaches maximum values and they are made up of fine and coarse materials. The
252 distal part is the most complex. Debris fans are deposited by debris flow, while boulders and

253 finer debris are scattered and boulder accumulations with sliding fabric are the most common
254 feature.
255 The thermal regime shows a large difference between the ground and the air (Table 1). In the
256 lower part of the cones and walls the AAMT is around 2.4ºC higher than in the upper areas
257 with an increase in the Freezing Index from moderate to intense (208 points) and 20 more
258 freeze/thaw cycles. The ground temperature, recorded at 1865 m a.s.l., shows higher AGMT,
259 a very low Freezing Index and hardly any freeze/thaw cycles. The ground thermal regime
260 indicates a strong dependence on the snow cover, such that only in years with a thin or short-
261 lasting snow cover did temperatures reach -1ºC/-2ºC (Pisabarro et al. 2017).
262 The duration of the snow cover over the seven years studied was highly variable, between two
263 months in 2012 and seven months in 2013, as is common in the wet and moderately cold high
264 mountain (AAMT, 6ºC at 1800 m a.s.l.). The high variability of the snow cover and
265 moderately low temperatures mean high thermal variability on the ground, melt processes and
266 surface water flow during the winter period. Slab avalanches are very frequent, around 10 per
267 year over the study period. They have no geomorphological effects but lead to snow over-
268 accumulation and a late melt in the lower parts of the debris talus and cones with important
269 implications for the ground thermal regime.
270 Table 1
271 The freeze and frost shattering affects the walls, which remained free of snow in all years,
272 whereas on the debris cones this was minimal due to the low altitude and snow protection.
273 Thus, cryogenic processes have a very modest presence in the cones analyzed.
274 - **Scree accumulation and processes**. Large landslides or rockfalls have not been detected on
275 the cones studied since 1946, only debris flow events reworking the existent features. On the
276 SE face a photograph taken by H. Obermaier in 1914 shows the slopes occupied by blocks
277 and debris while the plain is free of them, but by 1946 debris covered 60.5% of the surface of

278 the plain and slopes. Ten years later a large rockfall of 46,000 m^2 covered half the plain,
279 showing sliding on the snow. A photograph taken by E. Hernández-Pacheco (1956) shows
280 very fresh deposits. Three large rock falls were detected between 1940 and 2005 (two
281 between 1940 and 1956, and one in 2004-2005) with a minimum recurrence of 0.04 events
282 per year. The last rockfall was a small one of 1,000 m^2 between 2003 and 2005 when the area
283 occupied by debris reached 97% of the intramoraine plain (Figure 4). Accumulation rates on
284 the wall base show a fall in activity in the walls since the mid-twentieth century.
285 Only debris flow features and a small rock fall were detected on the cones studied between
286 1946 and 1981. The debris flow events continued over the following ten years, but there were
287 only two debris flows in C-2 and C-1 over the nine years of observations, and there have been
288 a minimum of 14 events recorded in the last 70 years (0.19 events per year). Observation of
289 snow avalanches over the last 10 years shows there are very common successive annual
290 events, predominantly slab avalanches and wet dirty snow avalanches in spring. They reach
291 the proximal and middle parts every year, though snow avalanches can also carry boulders
292 and fine sediments to distal parts.
293 Figure 4
294 **Volumetric changes on debris cones**
295 Annual volumetric changes (Figure 5) detected by the TLS survey on debris cones 1 and 2
296 (Table 2) show considerable variability over the five years analyzed (Table 2) and net
297 differences in sediment redistribution on the cones.
298 Table 2
299 - **Cone A** presents a steep slope (33º-35º) and straight-line morphology (Figure 6A). Annual
300 changes in volume show alternation between loss and increase. Increased volume coincides
301 with years of stable snow cover and volume loss with unstable snow cover. Total volume
302 change shows a moderate increase in sediments, 121,22 m^3 over five years. The behavior by

parts shows clear differences (Figure 5, Table 2). In the middle and proximal parts the accumulation is greater than in the distal one. In the proximal part the accumulations overlap with the deepest incisions linked to the debris flow channel where incisions of around a meter take place. The proximal part is fed by rockfalls and snow avalanches and shows moderate sediment input. The middle part is where the accumulation is greater, showing thickening of around 34%, which is 9 times greater than in the distal part. Longitudinal structures are interpreted as displacement by debris lobes and though the coarsest materials are transported mainly by debris flow, the debris lobes are predominant. The middle and proximal parts contain 71% of the areas with thickening. In 2013-2014 a debris flow event brought about a moderate channel incision (25-50 cm). The distal part shows the highest volume loss rates, mainly in the central and eastern parts. The materials go down towards two dolines, partially filled by boulders and fine sediments.

Figure 5.

As a whole, the volume loss rates for the entire cone are between 0.5 and 25 cm^3, the highest appearing in the central and eastern parts where the lobes and debris flow indicate greater morphogenetic activity (Figure 3, C and D). The longitudinal structures point to the redistribution of dominant processes from the proximal part, where material accumulates by rock fall and snow avalanches with accumulation rates of 2,74 mm a^{-1} towards the distal part moved by debris lobes on 86% of the surface and by debris flow on the remaining 14%. Changes detected in the debris lobes are around 0-25 cm thick in 2010-2011, 2011-2012 and 2013-2014. The largest thicknesses in the longitudinal structures are detected in 2010-2011, when changes of less than 0.50 cm are dominant, though changes between 0.50-100 cm are common (Figure 5). Volume increase is estimated as a minimum sediment input of 24 m^3 a^{-1}.

Figure 6

- **Cone B** possesses a concave-convex profile with a slope of 33º-35º becoming more moderate at the distal part (29º) (Figure 6A). The data show accumulation between 2009 and

2011 and volume loss in 2012-2013 without a direct link to the snow cover changes (Figure 5). The total volume change shows an increase in sediments of 4,642 m^3 over five years and negative values are only found in 2012-2013 (2C). The proximal part shows an increase of >50-100 cm while the main changes were detected in the middle part, where volume loss is dominant (Figure 6). In the proximal part, deep incisions in the debris flow channel show changes in net accumulation or erosion (50->100 cm) together with boulder increase. In the middle part thickening is 18 times greater than in the distal part. The middle and proximal parts contain 84% of the areas with thickening. (Table 2). The five-year trend showed a net accumulation of 1,588.41 m^3 linked to rock fall and snow avalanches with an accumulation rate of 35.5 mm a^{-1}.

The negative values, corresponding to volume loss, are concentrated in the debris flow areas with changes of around 25-100 cm a^{-1}. Thickening is dominant, the data showing between 0,2 and 50 cm with the largest changes appearing in the debris flow channels, which were infilled by more than 1 meter of debris between 2009-2010 and 2011-2012. Measurements of the boulder fabric indicate (Figure 7) dominance of sliding fabric as a result of rockfall over snow cover in spite of the transversal orientation of 20% of the boulders. In the middle part longitudinal orientations and sliding fabric are dominant, linked to the presence of debris lobes. The rolling fabric boulders from rockfalls or snow avalanches reach the middle part, where there are longitudinal and transversal structures and accumulation rates have been estimated at 36.88 mm $a^{-1.}$ The transversal structures show undulations of around 50->100 cm in areas of boulder accumulation with dominance of sliding fabric (Figure 7). This organization coincides with mass movements such as slope slide and shallow slide-earthflow, indicating a change of process in the distal part. The presence of slides may be attributed to slopewash and settling, helped by water availability and sediment output.

Figure 7.

Changes in total cone volume were homogeneous in 2009-2010, 2010-2011 and 2013-2014, with an abrupt change in 2012-2013 when positive deformations doubled, and in 2012-2013 when the value was moderately negative at -663 m^3. Cone B, in the debris flow area, has volume loss rates of around 50-100 cm (Figure 3 E). During the five years volumes increased and, although variability was high, a minimum input sediment of 928 m^3 a^{-1} is estimated, equivalent to 26.2 mm a^{-1}.

From top to bottom Cone B shows different processes (Figure 8: at the top rockfall and debris flow are dominant, in the middle creep develops debris lobes with longitudinal structures and in the distal part slow slide earthflow, slope wash and setting deforming the profile and generating transversal structures. Figure 7C shows the dynamic differences between the two cones. Cone A loses volume in the proximal area and accumulates moderately in the distal, whereas Cone B presents net accumulation in the proximal area, loss of volume in the middle and net accumulation in the distal.

Figure 8

4. Discussion

The processes involved in the debris dynamic imply feeding on the talus and the displacement of clasts over the talus. At first the feed of clasts came from the walls and the vertical rock channel crossing the walls and the debris accumulations where a wide range of processes and changes have been detected from the proximal to the distal parts. Rapp (1960) defined four types of processes: subsidence, talus creep, individual rolling, and small slides, and later debris shift and debris flow were included as determinant processes (Gardner, 1968,1983; Van Steijn,1988 Luckmann, 2013b), all of them transferring the sediments and reworking the morphology of the cones by increasing or reducing their volume by sectors. Processes referred to as "talus creep" by A. Rapp (1960) are related to the presence of ice on the ground, and Van Steijn (1988) referred to "debris shift" as a wide variety of processes.

379 The recognition of different types of slope processes as individual or related events (Figure 8)
380 helps to provide an understanding of debris transfer mechanisms in slopes and debris cones
381 (Luckmann, 1988, 2013b; Van Steijn, 2002). In the Rocky Mountains, Moore et al. (2009)
382 proposed that the segregation of ice is not a determinant agent, so mechanisms such as
383 topographic or tectonic stress and also paraglacial dynamics must be taken into account. Hales
384 and Roering (2005) in the New Zealand Alps point to the local relief, the erosion linked to
385 faulting or jointing and the slope dip as the most significant factors. Most of the studies on the
386 dynamics of debris cones are related to the presence of permafrost or seasonal ice, but in the
387 temperate high mountain the large talus and debris cones are located at low altitude in
388 environments without seasonal ice and with a winter snow cover that protects the ground from
389 frost. The moderate freezing index and low annual freeze/thaw cycles (20-50, Pisabarro et al.
390 2017) favor physical weathering on the walls, located for three months per year at the lower
391 limit of the frost cracking window (-3 to -5ºC), where temperatures are between -6 and -3ºC,
392 the range most sensitive to frost cracking in limestone (Matsuoka, 2001). At present, the low
393 freezing index means that these processes are not determinant in the accumulation of clasts at
394 the foot of the walls (Pisabarro et al. 2017). As in the Rocky Mountains (Moore et al., 2009),
395 in the Picos de Europa the processes of rock mass strength coinciding with a tectonic line, a
396 fracture and thrust, determine variations in rockfall production. Measurements have been
397 taken on debris lobes on the north face of Peña Vieja at 2437 m a.s.l. and Tesorero peak at
398 2320 m a.s.l. The displacement estimated on Peña Vieja was 0.23/0.31 cm a^{-1} and on Tesorero
399 slope between 1.88 and 1.41 cm a-1 (Brosche, 1994), both understood as gelifluction lobes
400 with frost action though located above the cones studied and both north oriented.
401 On the eastern side changes have been frequent at the foot of the 500 m high walls on a plain
402 enclosed by a moraine (Figure 4) attributed to the Dryas (Serrano et al. 2012, 2017), where
403 the scree feed is linked to a large debris fall and debris flow, and climate-determined

variations can take place in scree production. The study area would have been entirely deglaciated at the end of the Younger Dryas around 11 ka (Serrano et al. 2013) and thrust emplacement and paraglacial strength may be the determinant factors in the effectiveness of rock fall processes but also periglacial ones on walls during cold stadia.

The measurements using TLS indicated moderate annual changes of between 2 and 50 cm, mainly by the redistribution of fall material by debris flows and snow avalanches, but not by feed from the walls.

The organization of debris cones is characterized by the dominance of accumulation in the proximal part with intense erosion processes caused by debris flow events and significant annual changes. The low intensity-high frequency nivation processes shifts clasts downslope. Rockfall, debris flow, and snow avalanches bring fine and coarse sediments to the middle parts and generating longitudinal lobes and boulder alignment. The debris cone can therefore be considered as subsystem II in the sediment cascade concept, in which the sediments are stored and reworked (Davies and Korup, 2010).

On the debris cones can be distinguished minor morphogenetic subsystems because changes in processes, structures and accumulation rates. Both cones show the same dynamic by parts (proximal, middle and distal, Figures 5 and 6). The most active processes are located in the proximal (accumulative) and the distal parts. The behavior of the two cones was the opposite of one another in three of the five years observed (Figure 5 and 6, Table 2). Cone B was more active and unstable with higher accumulation rates and annual variability affecting 8.7% of its surface, while only 0.54% of Cone A was affected by annual changes. There are no visible trends over the five years studied, although in 2012-2013 both cones lost volume and in 2013-2014 both increased in volume. Sediment transfer inside the cones was responsible for the cone profile and brought on linked processes between the proximal and middle parts and the middle and distal ones.

- **The proximal part** shows alternate thinning and thickening. Rock fall and snow avalanches bring fine and coarse sediments with boulders that reach the middle part of the cones. Van Steijn (2002) showed that the cones correspond to slow evolution, with massive deposits characterized by century recurrences and highly episodic processes such as rockfall, debris flows, and snow avalanching, in a high magnitude-low frequency system.

The transversal orientations of the boulders indicate the origin of boulders from snow avalanches in the middle parts. Dirty snow avalanches only reach the distal parts in extraordinary events.

Debris flows are the most efficient process in modifying the upper part, but to a greater extent also the middle and distal parts. This has been well studied often in association with the melt of the active layer in permafrost environments, but also related to snow avalanches and swift snow melt or intense precipitations (Decaulne and Saemundsson, 2006). The abundance of fine sediments in the proximal part is critical in facilitating debris flow in the high parts of cones (Hinchliffe et al., 1998). In La Vueltona, snow patches persist until July-August saturating the debris deposits in the apex. Intense precipitation and melt from snow patches support the rapid water availability on partially saturated deposits and the genesis of debris flow along pre-existing channels. The known debris flows during the last ten years are all linked to intense rainfall.

The minimum recurrence of debris flows estimated in the area studied is 0.19 events per year for the last seventy years, and in the debris cones a minimum recurrence of 0.2 events per year over the last ten years. In similar environments estimated recurrences are of 0.025 events per year in Swedish Lapland (Rapp and Nyberg, 1981), 0.15 events per year in the Rocky Mountains (Gardner, 1979), between 0.5 and 2.5 events per year in the Alps (Blijenberg, 1998) and 0.2-0.5 events per year in Iceland (Decaulne et al. 2005). Our data are in accordance with wet temperate environments in the Rocky Mountains and Iceland. The high

454 frequency of debris flow favor sediment transfer more than do snow avalanches in wet
455 environments with thick snow cover (Van Steijn, 2002).
456 - **The middle part** shows important changes of around 0.75-100 cm in Cone B. Scattered
457 large blocks and rolling fabric of the boulders point to the arrival of clasts by snow avalanches
458 and rockfalls, consistent with feeding by the denominated snow avalanche boulder tongue
459 transition deposits (Jomelli and Francou, 2000) rather than by rockfall. But in both cones the
460 dominant landforms in the middle part are the metric to decametric debris lobes together with
461 the debris flow channels. Creep is the main process in the redistribution of materials on the
462 debris cone surface, showing a longitudinal structure by thinning and thickening along the
463 slope. In the absence of frost, creep works through saturation by snow melt waters, as has
464 been established in other high mountains (Pérez, 1985, 1988). The dynamic of the debris
465 lobes is related to water availability by snow melt under the snow cover from March to July.
466 Accumulation of debris is moderate in Cone A (1.4 mm a^{-1}) and high in Cone B, which has
467 accumulations of 36.88 mm a^{-1}.
468 - **The distal part** is characterized by the accumulation of large boulders and digitate tongues
469 of debris flows. The distal part undergoes smaller volume changes and accumulation rates,
470 loss of volume, erosion and sediment output (figure 7) and the flow structures change
471 completely with transversal structures dominant. Debris lobes are less common and the open
472 work by slopewashing is unfavorable to their presence. Nevertheless, the transversal
473 structures are not consistent with the gradient of the slope. These structures have not
474 previously been analyzed in high mountain talus and cones, though Rapp (1960) pointed to
475 the presence of subsidence in the debris cones. The reactivation of distal slides and slow slide-
476 earth flow may be correlated to the presence of undetected seasonal ice in the area or to
477 washing and oversaturation causing local subsidence and slide processes in small depressions
478 (Figure 7). These distal movements may be consistent with gravitational and meltwater-

induced processes (creeping, sliding) taking place in alpine debris cones, predominantly at the lower end of the talus slopes, where concave-up slope profiles are sometimes generated (Kellerer-Pirklbauer and Kaufmann, 2007). Although these authors relate the processes to the presence of mountain permafrost, the supply of snowmelt water to the lower part of the cones may have the same consequences as those brought by the melting of frozen bodies. Whatever the case, in warm and wet mountains deformations by flow of possible frozen bodies must be discarded.

Accumulation rates point to changing values between the proximal part, where values are high in both cases, the middle part, with the higher values in Cone B and moderate ones in Cone A, and the distal one, where accumulation rates are less than 10 mm (Table 2). The accumulation and erosion rates are lower when the time interval is longer (Sadler, 1981; Gardner et al. 1987; Sanders, 2012) since the initial rate of scree deposition may be higher. As the debris accumulation may have begun 11 ka ago, erosion rates could have been higher than those of the present day. The estimated mean accumulation rates of between 1.6 and 26.21 mm a^{-1} are very different indicating a highly dynamic Cone B and a less active Cone A. Both are located at similar altitudes with similar climate conditions and environment. The very different rates show the importance of topography, tectonic setting, glacial erosion and nival processes rather than climate determined processes. As we previously pointed out (Sanders, 2012), under certain geological circumstances talus accumulation can develop in comparatively low topographic locations under warm climatic conditions. Accumulation rates are consistent with measurements in the temperate high mountain of the Rocky Mountains and the Alps, where accumulation rates have been estimated between 1 and 60 mm a^{-1} (Gardner, 1983; Luckmann, 1988; 2013b; Wieczorek et al., 2008; Sanders, 2012; Krautblater and Dickau, 2017;).

503 The present-day low accumulation rates in formerly glaciated areas have led to the suggestion
504 of a paraglacial origin linked to rapid accumulations when accelerated rockwall failures and
505 exposure to atmospheric conditions coincide following glacier recession (Ballantyne, 2002),
506 mainly reflecting a paraglacial environment in a wet mountain climate.

507 **5. Conclusion**

508 The TLS survey and geomorphological analysis applied on two debris cones in the humid
509 temperate mountains has facilitated data of annual topographic changes and transfer of
510 sediments from the walls (subsystem I) to the cones (Subsystem II) in the cascade sediments
511 concept. The combination of TLS and detailed scale geomorphological surveys has facilitated
512 the knowledge of the processes involved in the talus dynamic and the rates of change on the
513 slopes. The application of TLS has been effective in detecting the way debris and transversal
514 flows function, and in monitoring annual topographic changes, but if we wish to establish
515 trends more annual surveys must be conducted.

516 The mean accumulation rates of the talus are high, from 24.2 and 80.7 m^3 a^{-1}, but not too
517 much higher than mean accumulation rates of other scree accumulations in the temperate high
518 mountain. Changes in topography are around 50-100 cm a^{-1} at specific points, but active
519 debris lobes accumulate between 1.6-26.2 mm a^{-1} at altitudes between 1900 and 2200 m.

520 The air and ground temperature data show processes unrelated to frost on talus and cones,
521 where debris flows, snow avalanches, creep, and slides are the main processes involved in the
522 sediment transfer of subsystem II. Climatic conditions and geomorphic indicators as the
523 accumulation rates and processes permit us to propose a paraglacial environment linked to the
524 morphotectonic setting and a wet climate.

525 There is an equilibrium between accumulation and transfer of sediments in Cone A, whereas
526 in Cone B accumulation processes are dominant in the upper part and sediment transfer in the
527 distal one. the most important processes in the morphological evolution of debris cones in the

areas studied are four. Debris flow, which affects the proximal parts and reworks the medium and distal ones. Snow avalanches, which bring materials to the intermediate parts and only exceptionally to the lower ones. Creep, associated with snow melt and manifested through debris lobes. Finally, creep and slide earthflow linked to subsidence generate transversal structures in the low areas.

The debris cone dynamic is defined by the changeover from high intensity-low frequency processes (debris flow, avalanches) in the proximal part, to high frequency-low intensity ones (creep, shift, solifluction) in the middle and distal part, always crossed by downward debris flow.

Acknowledgments

This research was supported by the I+D+I CGL2015-68144-R (Ministerio de Economía y Competitividad) project (FEDER) and the Government of Extremadura (file number GR10071 FEDER).

References

Ballantyne, C.K., 2002. Paraglacial geomorphology. Quaternary Science Reviews 21, (18-19), 1935-2017.

Bauer, A., Paar, G., Kaufmann, V., 2003. Terrestrial laser scanning for rock glacier monitoring, in: M. Philips, S.M. Springth and L.U. Arenson (eds.), Proceedings of the 8ª International Conference on Permafrost. IPA, Zurich, pp. 55-60.

Becht, M., Haas, F., Heckmann, T., Wichmann, V., 2005. Investigating sediment cascades using field measurements and spatial modelling, In: Sediment Budgets (Proceedings of symposium S1, Seventh IAHS Scientific Assembly). IAHS Publ. 291, pp. 2006-2013.

Blijenberg, H.M., 1998. Application of physical modelling of debris flow triggering to field conditions: limitations posed by boundary conditions. Engineering Geology 91, 25-33.

552 Brosche, K.U., 1994. Ergbenisse von Abstragungsmessungen an periglazialen Solifluktions
553 schuttdecken in vier Hochgebirgen der Iberischen Halbinsel (the Picos de Europa, Peña
554 Prieta, Sierra de Urbión und Sierra Nevada). E&G Quaternary Science Journal 44, 28-55.
555 Caine, N. ,1969. A model for alpine talus slope development by slush avalanching. Journal of
556 Geology 77 (1), 92-100.
557 Caine, N., 1974. The geomorphic processes of the alpine environment, In: J. D. Ives, R. G.
558 Barry (eds.), Arctic and Alpine Environments. Methuen, London, pp.721-748.
559 Castañón, J.C., Frochoso, M., 1994. El periglaciarismo de la Cordillera Cantábrica, In:
560 Gómez Ortiz, M. Simón Torres, F. and Salvador Franch, F.(eds.), Periglaciarismo en la
561 Península Ibérica, Canarias y Baleares. Estudios significativos. SEG, Granada, pp.75-91.
562 Castañón, J.C., Frochoso, M., 1998. La alta montaña cantábrica: condiciones térmicas y
563 morfodinámica en los Picos de Europa, In: A. Gómez Ortiz, M. Salvador Franch, F.
564 Schulte and L. García-Navarro, A (eds), Procesos biofísicos actuales en medios fríos.
565 Universidad de Barcelona, Barcelona, pp. 113-132.
566 Davies, T.R.H., Korup, O., 2010. Sediment cascades in active landscapes, In: T. Burt, J.R.
567 Allison, (eds.), Sediment cascades: an integrated approach. Wiley-Blackwell, Oxford, pp.
568 89-116.
569 Decaulne, A., Sæmundsson, O., 2006. Geomorphic evidence for present-day snow-avalanche
570 and debris-flow impact in the Icelandic Westfjords. Geomorphology 80, 80–93.
571 Decaulne A., Sæmundsson, O., 2010. Distribution and frequency of snow-avalanche debris
572 transfer in the distal part of colluvial cones in Central North Iceland. Geogrphiska Annaler
573 92 A, 177–187.
574 Decaulne, A., Saemundsson, Th., Petursson, O., 2005. Debris flows triggered by rapid
575 snowmelt in the Gleidarhjalli area, northwestern Iceland. Geografiska Annaler 87A, 487-
576 500.

577 Delaloyé, R., Reynard, E., Lambiel, C., Marescot, L., Monnet, R., 2003. Thermal anomaly in
578 a cold scree slope, Creux du Van, Switzerland, In: M. Philips, S.M. Springth, L.U. Arenson
579 (eds.), Proceedings of the 8ª International Conference on Permafrost. IPA, Zurich, pp. 175-
580 180.
581 De Haas, T., Kleinhans, M. G., Carbonneau, P. E., Rubensdotter, L., Hauber E., 2015. Surface
582 morphology of fans in the high-Arctic periglacial environment of Svalbard: controls and
583 processes. Earth-Science Reviews 146, 163–182.
584 Farias, P., 1982. La estructura del sector central de los Picos de Europa. Trabajos de Geología
585 12, 63-72.
586 Fengqing, J., Yanwei, Z., 2011. Freezing and thawing index, in: V.P. Singh, P. Singh, U.
587 Haritashya, (eds.), Encyclopedia of snow, ice and glaciers. Springer, Dordrecht, pp. 301.
588 Fey, C., Wichmann, V., 2017. Long-range terrestrial laser scanning for geomorphological
589 change detection in alpine terrain-handling uncertainties. Earth Surface Processes and
590 Landforms 42, 789-802.
591 Francou, B., 1983. Géodynamique des dépots de pied de paroi dans l´etage périglacial. Revue
592 de Géologie Dinamique et Geographie Physique 24 (5), 411-424.
593 Francou, B., 1988. L'Eboulisation en Haute Montagne. Editec. Grenoble.
594 Francou, B., 1991. Pentes, granulométrie et mobilité le long d'un talus d'éboulis en milieu
595 alpin. Permafrost and Periglacial Processes 2, 175-186.
596 French, H.M., 2007. The periglacial environment. Wiley and Sons, Chichester.
597 Gardner, J.S., 1968. Debris slope form and processes in the Lake Louise District: a high
598 mountain area. Department of Geography, McGill University, Montréal.
599 Gardner, J.S., 1979. The movement of material on debris slopes in the Canadian Rocky
600 Mountains. Zeitschrift fur Géomorphologie 23, 45-67.

601 Gardner, J.S., 1983. Accretion rates on some debris slopes in the Mt. Rae Area, Canadian
602 Rocky Mountains. Earth Surface Processes and Landforms 8 347-355.
603 Gardner, J.S., 1983. Observations on erosion by wet snow avalanches, Mount Rae area,
604 Alberta, Canada. Arctic and Alpine Research 15, 271-274.
605 Gigli, G., Morelli, S., Fornera, S., Casagli, N., 2014. Terrestrial laser scanner and
606 geomechanical surveys for the rapid evaluation of rock fall susceptibility scenarios.
607 Landslides 11(1), 1-14.
608 González-Trueba, J.J. , 2007a. El paisaje natural del Macizo Central de los Picos de Europa.
609 CIMA, Consejería de Medio Ambiente, Santander.
610 González-Trueba, J.J., 2007b. Geomorfología del Macizo Central del Parque Nacional de
611 Picos de Europa. OAPN-Ministerio de Medio Ambiente, Madrid.
612 González-Trueba, J.J., Serrano, E., 2010. Geomorfología del Macizo Oriental del Parque
613 Nacional de Picos de Europa. OAPN-Ministerio de Medio Ambiente, Madrid.
614 Götz, J., Otto, J.C., Schrott, L., 2013. Postglacial sediment storage and rockwall retreat in a
615 semi-closed inner-alpine basin (Gradenmoss, Hohe Tauern, Austria). Geografia Fisica e
616 Dinamica Quaternaria 36 (1), 63-80.
617 Goudie, A., 1981. Geomorphological Techniques. Allen & Unwin, London.
618 Hales, T. C., Roering, J. J., 2005. Climate-controlled variations in scree production, Southern
619 Alps, New Zealand. Geology 33(9), 701-704.
620 Herz, T., King, L., Gubler, H., 2003. Microlimate whithin coarse debris of talus slopes in the
621 alpine periglacial belt and its effect on permafrost, in: M. Philips, S.M. Springth and L.U.
622 Arenson (eds.), Proceedings of the 8ª International Conference on Permafrost. IPA, Zurich,
623 pp. 383-388.

624 Hinchliffe, S., Ballantyne, C.K., Walden J., 1998. The structure and sedimentology of relict
625 talus, Trotternish, northern Skye, Scotland. Earth Surface Processes and Landforms 23,
626 545-560.
627 Jomelli, V., Francou, B., 2000. Comparing characteristics of rockfall talus and snow
628 avalanche landforms in an alpine environment using a new methodological approach.
629 Geomorphology 35, 181-192.
630 Kellerer-Pirklbauer, A., Kaufmann, V., 2007. Paraglacial talus slope instability in recently
631 deglaciated cirques (Schober Group, Austria). Grazer Schriften der Geographie und
632 Raumforschung 43, 121-130.
633 Kirkby, M., Statham, I., 1975. Surface stone movement and scree formation. Journal of
634 Geology 83(3), 349-362.
635 Kotarba, A., Kaszowski, L., Krzemien, K., 1987. High mountain denudational system of the
636 Polish Tatra Mountains. Polish Academy of Science, Kracow.
637 Kotarba, A., Klapa, M., Midriak, R., Petras, J., Skroda, J., 1979. Field experiments on high
638 mountain slopes of the Tatra Mts. Studia Geomorphologica Carpatho-Balcanica 13, 132-
639 148.
640 Krautblatter, M., Dikau, R., 2007. Towards a uniform concept for the comparison and
641 extrapolation of rockwall retreat and rockfall supply. Geografiska Annaler 89A, 21-40.
642 Luckman, B.H., 1976. Rockfalls and rockfall inventory data: some observations from Surprise
643 Valley, Jasper National Park, Canada. Earth Surface Processes and Landforms 1, 287-298.
644 Luckman, B.H., 1988. Debris accumulation patterns on talus slopes in Surprise Valley,
645 Alberta. Géographie Physique et Quaternaire 42 (3), 247-278.
646 Luckman, B.H., 2013a. Processes, transport, deposition and landforms: rockfall, in: J.
647 Shroder, R.A. Marston, M. Stoffel (eds.), Treatise on Geomorphology, vol. 7, Mountain
648 and Hillslope Geomorphology. Academic Press, San Diego, pp. 174-182.

649 Luckman, B.H., 2013b. Talus Slopes, in: S.A. Elias (ed.), The Encyclopedia of Quaternary
650 Science. Elsevier, Amsterdam, pp. 566-573.
651 Marquínez, J., 1989. Síntesis cartográfica de la región del Cuera y los Picos de Europa.
652 Trabajos de Geología 18, 137-144.
653 Marquínez, J., 1992. Tectónica y relieve en la Cornisa Cantábrica, in: A. Cearreta, F.M.
654 Ugarte (eds.), The late Quaternary in the western Pyrenean region. Universidad del País
655 Vasco, Vitoria, pp. 143-160.
656 Moore, J.R., Sanders, J.W., Dietrich, W.E., Glaser, S.D., 2009. Influence of rock mass
657 strength on the erosion rate of alpine cliffs. Earth Surface Processes and Landforms 34,
658 1339-1352.
659 Otto, J.C., Schrott, L., Jaboyedoff, M., Dikau, R. 2009. Quantifying sediment storage in a
660 high Alpine valley (Turtmanntal, Switzerland). Earth Surface Processes and Landforms 34
661 (13), 1726-1742.
662 Pérez, F.L., 1988. The movement of debris on a high Andean talus. Zeitschrift für
663 Geomorphologie 32, 77-99.
664 Pérez, F.L., 1993. Talus movement in the high equatorial Andes: a synthesis of ten years of
665 data. Permafrost and Periglacial Processes 4, 199-215.
666 Pérez, F.L., 1998. Talus fabric, clast morphology, and botanical indicators of slope processes
667 on the Chaos Crags (California Cascades), USA. Géographie Physique et Quaternaire 52
668 (1), 1- 22.
669 Pisabarro, A., Pellitero, R., Serrano, E., Gómez-Lende, M., González-Trueba, J.J., 2017.
670 Ground temperatures, landforms and processes in an Atlantic mountain. Cantabrian
671 Mountains (Northern Spain). Catena 149, 623-636

672 Phillips, M., Mutter, E.Z., Kern-Luetschg, M., Lehning, M., 2009. Rapid degradation of
673 ground ice in a ventilated talus slope: Flüela Pass, Swiss Alps. Permafrost and Periglacial
674 Processes 20, 1-14.
675 Rapp, A., 1960. Recent development of mountain slopes in Karkevagge and surroundings,
676 northern Scandinavia. Geografiska Annaler 42, 65-200.
677 Rapp, A., Fairbridge, R.W., 1968. Talus fan or cone, in: R.W. Fairbridge (ed.), Encyclopaedia
678 of Geomorphology. Van Nostrand Reinhold, New York. pp. 1106-1109.
679 Rapp, A., Nyberg, R., 1981. Alpine debris flows in northern Scandinavia: morphology and
680 dating by lichenometry. Geografiska Annaler 63A, 183-196.
681 Rosser, N.J., Petley, D.N., Lim, M., Dunning, S.A., Allison, R.J., 2005. Terrestrial laser
682 scanning for monitoring the process of hard rock coastal cliff erosion. Quarterly Journal of
683 Engineering Geology and Hydrogeology 38, 363–376.
684 Sadler, P.M., 1981. Sediment accumulation rates and the completeness of stratigraphic
685 sections. Journal of Geology 89, 569-584.
686 Sanders, D., Ostermann, M., Kramers, J., 2009. Quaternary carbonate-rocky talus slope
687 successions (Eastern Alps, Austria): sedimentary facies and facies architecture. Facies 55,
688 345-373.
689 Sanders, D., 2012. Talus accumulation in detachment scars of Late Holocene rock avalanches,
690 Eastern Alps (Austria): rates and implications. Géologie Alpine 9, 82-99.
691 Sanjosé, J.J., Berenguer, F., Atkinson, A.D.J., De Matías, J., Serrano, E., Gómez-Ortiz, A.,
692 González-García, M., Rico, I., 2014. Geomatics techniques applied to glaciers, rock
693 glaciers and ice-patches in Spain (1991-2012). Geografiska Annaler 96A, 307-321.
694 Scapozza, C., Lambiel, C., Baron, L., Marescot, L., Reynard, L., 2011. Internal structure and
695 permafrost distribution in two alpine periglacial talus slopes, Valais, Swiss Alps.
696 Geomorphology 132, 208-221.

Schrott, L., Adams, T., 2002. Quantifying sediment storage and Holocene denudation in an Alpine basin, Dolomites, Italy. Zeitschrift für Geomorphologie 128, 129-145.

Schrott, L., Hufschmidt, G., Hankammer, M., Hoffmann, T., Dikau, R., 2003. Spatial distribution of sediment storage types and quantification of valley fill deposits in an Alpine basin, Reintal, Bavarian Alps, Germany. Geomorphology 55, 45-63.

Selby, M.J., 1983. Hillslope, materials and processes. Oxford University Press, Oxford.

Serrano, E., González-Trueba, J.J., 2004. Morfodinámica periglaciar en el grupo Peña Vieja (Macizo Central de los Picos de Europa -Cantabria-). Cuaternario y Geomorfología 18, 73-88.

Serrano, E., González-Trueba, J.J., Sanjosé, J.J., Del Río, L.M., 2011. Ice patch origin, evolution and dynamics in a temperate high mountain environment: the Jou Negro, Picos de Europa (NW Spain). Geografiska Annaler 93, 57-70.

Serrano, E., González-Trueba, J.J., González-García, M., 2012. Mountain glaciation and paleoclimate reconstruction in the Picos de Europa (Iberian Peninsula, SW Europe). Quaternary Research 78, 303-314.

Serrano, E., González-Trueba, J.J., Pellitero, R., González-García, M., Gómez- Lende, M., 2013. Quaternary glacial evolution in the Central Cantabrian Mountains (Northern Spain). Geomorphology 196, 65-82.

Serrano, E., González-Trueba, J.J., Pellitero, R., Gómez-Lende, M., 2017. Quaternary glacial history of the Cantabrian Mountains of northern Spain: a new synthesis, in: P.D. Hughes and J.C. Woodward (eds.), Quaternary Glaciation in the Mediterranean Mountains. Geological Society, Special Publications, 433, London, pp. 55-85.

Statham, I., 1976. A scree slope rockfall model. Earth Surface and Processes 1, 43-62.

720 Thorn, C.E., Schlyter, P.L., Darmody, R.G., Dixon, J.C., 1999. Statistical relationships
721 between daily and monthly air and shallow-ground temperatures in Kärkevagge, Swedish
722 Lapland. Permafrost and Periglacial Processes 10, 317-330.
723 Van Steijn, H., de Ruig, J. Hoozemans, F., 1988. Morphological and mechanical aspects of
724 debris flows in parts of the French Alps. Zeitschrift für Geomorphologie 32, 143–161.
725 Van Steijn, H., Boelhouwers, J., Harris, S., Hétu, B., 2002. Recent research on the nature,
726 origin and climatic relations of blocky and stratified slope deposits. Progress in Physical
727 Geography 26, 551–575.
728 Wheaton, J.M., Brasington, J., Darby, S.E., Sear, D.A., 2010. Accounting for uncertainty in
729 DEMs from repeat topographic surveys: improved sediment budgets. Earth Surface
730 Processes and Landforms 35, 136–156
731 Vere, D., Mathews, J., 1985. Rock glaciers formation from a lateral moraine at
732 Bukkeholsbreen, Jotunheimen, Norway: a sedimentological approach. Zeitschrift für
733 Geomorphologie 29, 397-415.
734 Wieczorek, G.F., Stock, G.M., Reichenbach, P., Snyder, J.B., Borchers, J.W., Godt, J.W.,
735 2008. Investigation and hazard assessment of the 2003 and 2007 Staircase Falls rock falls,
736 Yosemite National Park, California, USA. Natural Hazards and Earth System Science 8,
737 421-432.
738 **Figures:**
739 Figure 1. Location of the studied area. Red dots indicate the meteorological stations (1, Upper
740 cable car station. 2, Cabaña Verónica station).
741 Figure 2. Up, geomorphological sketch of Peña Vieja Group and surrounding. Number 1 is
742 the debris cone A and number 3 is the debris cone B. Down, detailed geomorphological
743 sketch of debris cones A and B.

744 Figure 3. Debris cones in the Peña Vieja Group, where it is perceptible the relation between
745 wall unevenness and cones development. A. Southwest side, La Vueltona area, 1 and 3 are the
746 studied debris cones A and B. B. Southeast side, Áliva area, debris cones have less
747 development than in the other side. C. Cone B, detail of the surface morphology, debris lobes
748 (L), in the central portion, and debris flow features. D. Debris cone B, note the texture of
749 debris flow channel and fan, and the profile with debris lobe (L). Dfc, debris flow channel.
750 Dfa, debris fan. E, detail of debris fan in debris cone B.
751 Figure 4. Scree infill in the cirque SE of Peña Vieja-Áliva (1946-2014).
752 Figure 5. A. Topographic changes in Cone A (number 1 in Figure 2) and Cone B (number 3 in
753 Figure 2).
754 Figure 6. A, profiles of the cones A and B. B, year on year evolution of volume changes (m^3)
755 and accumulation rates (mm a^{-1}) in debris cones A and B. C, accumulation rates by parts and
756 surface of debris cones A and B.D, vertical changes at different radial distances from the apex
757 (a) Percentiles 25, 50 and 75 for vertical changes experiences by locations in cone A (a) and
758 cone B (b) at different radial distances from the apex.
759 Figure 7. A. Axe L boulder orientations in Cone B by altitude areas. d, slope direction.
760 Representation in percentage. B. Location of represented points in the profile of cone B. C.
761 Slow mass wasting in the distal part of debris cone B. D. Detail of lobes and flow direction
762 where the surface structure visible in TLS diagrams show transversal structures to flow
763 direction.
764 Figure 8. Toposequence of Debris cone B, with representation of processes, landforms and
765 deposits.
766 **Tables:**
767 Table 1. Climatic data of meteorological station and ground thermal records.

768 Table 2. Morphometric data (A), Volume and height changes by years (B), and changes by

769 sections (C) on debris cones of La Vueltona (2009-2014).

Table 1

Click here to download Table: ESC Table 1.docx

Table 1. Climatic data of meteorological station and ground thermal records.

Station	Type	Altitude m a.s.l.	MAAT ºC	Freezing Index	Frezee/thaw cycles	
					Nº	Period
Verónica*	Atmospheric	2325	3,6	390	20-50	October-April
El Cable*	Atmospheric	1823	6	178	20-30	October-April
Lloroza	Ground	1865	6,3	55	8	December-March

* Authomatic meteorological stations, OAPN. MAAT, mean annual air temperature.

Table 2

Click here to download Table: ESC Table 2.docx

Table 2. Morphometric data (A) Volume and height changes by years (B) and changes by sections (C) on debris cones of La Vueltona (2009-2014).

Cone			A				B			
Morpho-metric data	Extent	m^2	14866.00				35420.75			
	Length	m	360				410			
	Width	m	150				280			
	Altitude	m a.s.l	2200				2210			
			1990				1935			
	Freezing Index		0.75				0.83			
	Total Change	m^3	121.22				4642.03			
	Volume Increase	$m^3\ a^{-1}$	24.24				80.70			
Volume and height changes by years	2009-2010	m^3	-2407				1074			
		m	-161.91				30.32			
	2010-2011	m^3	2568				970			
		m	172.74				27.38			
	2011-2012	m^3	454				2174			
		m	30.53				61.37			
	2012-2013	m^3	-2195				-663			
		m	- 147.65				-18.71			
	2013-2014	m^3	1701				1090			
		m	114.42				30.77			
Changes by sections	Area		P	M	D	T	P	M	D	T
	Counted points		12244	25737	21,483	59,464	35,693	50,422	55568	14168
	Area	m^2	3061	6434.2	5370.7	14866.0	8,923.2	12,605.5	13892.0	35420.7
	Mean	m^3	0.0034	0.0017	0.0015	--	0.0445	0.0461	0.0131	--
	STD		0.045	0.031	0.039	--	0.171	0.455	0.108	--
	Volumen	m^3	42.04	45.16	34.01	121.22	1588.41	2324.63	728.99	4642.03
	Height	mm	13.73	7.018	6.332	8.154	178.00	184.41	52.47	131.05
	Height	$mm\ a^{-1}$	2.74	1.40	1.26	1.63	35.50	36.88	10.49	26.21

STD, Standard deviation. P, proximal. M, medial. D, distal. T, total.

Figure 1

Click here to download high resolution image

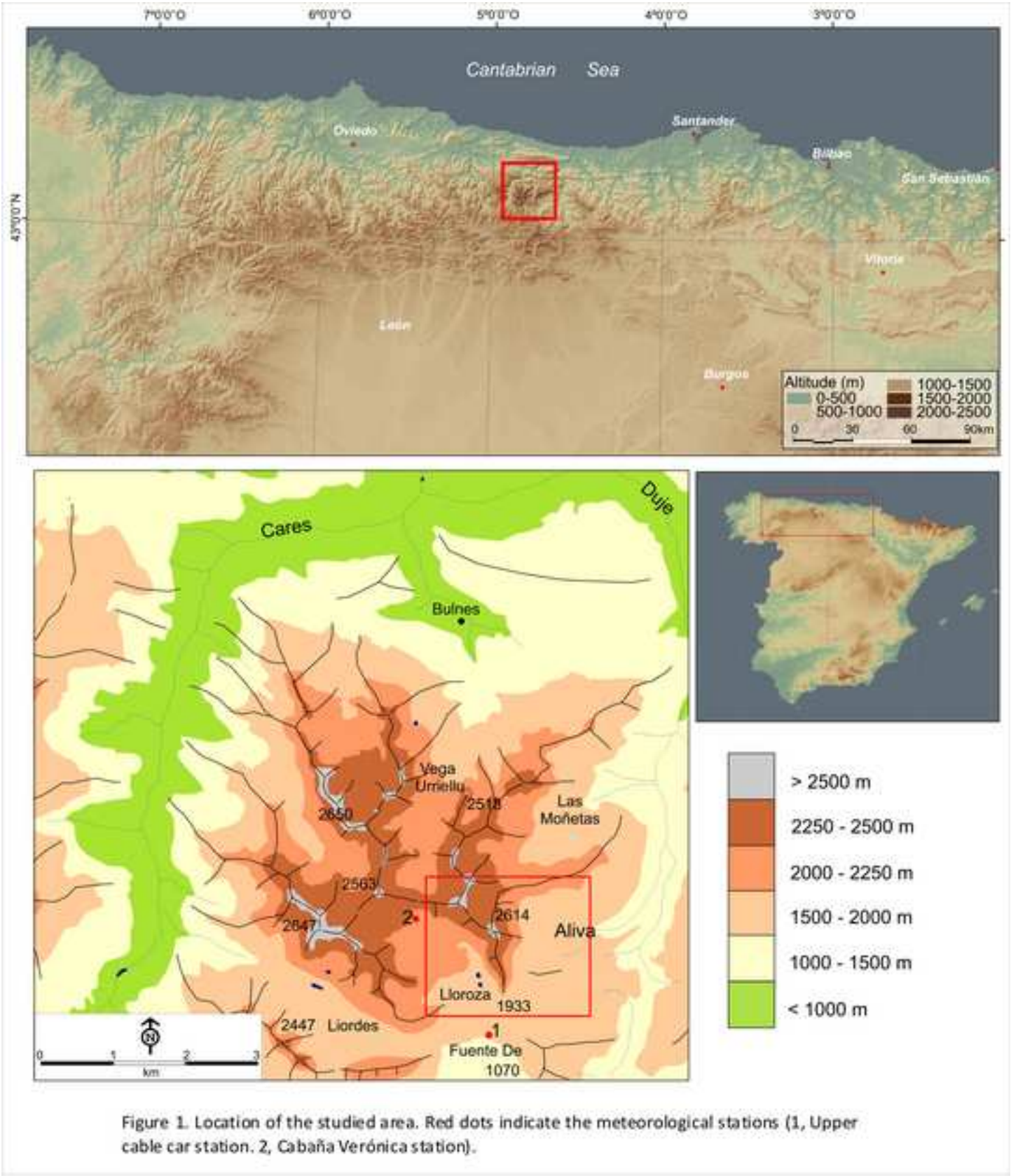

Figure 1. Location of the studied area. Red dots indicate the meteorological stations (1, Upper cable car station. 2, Cabaña Verónica station).

Figure 2

Click here to download high resolution image

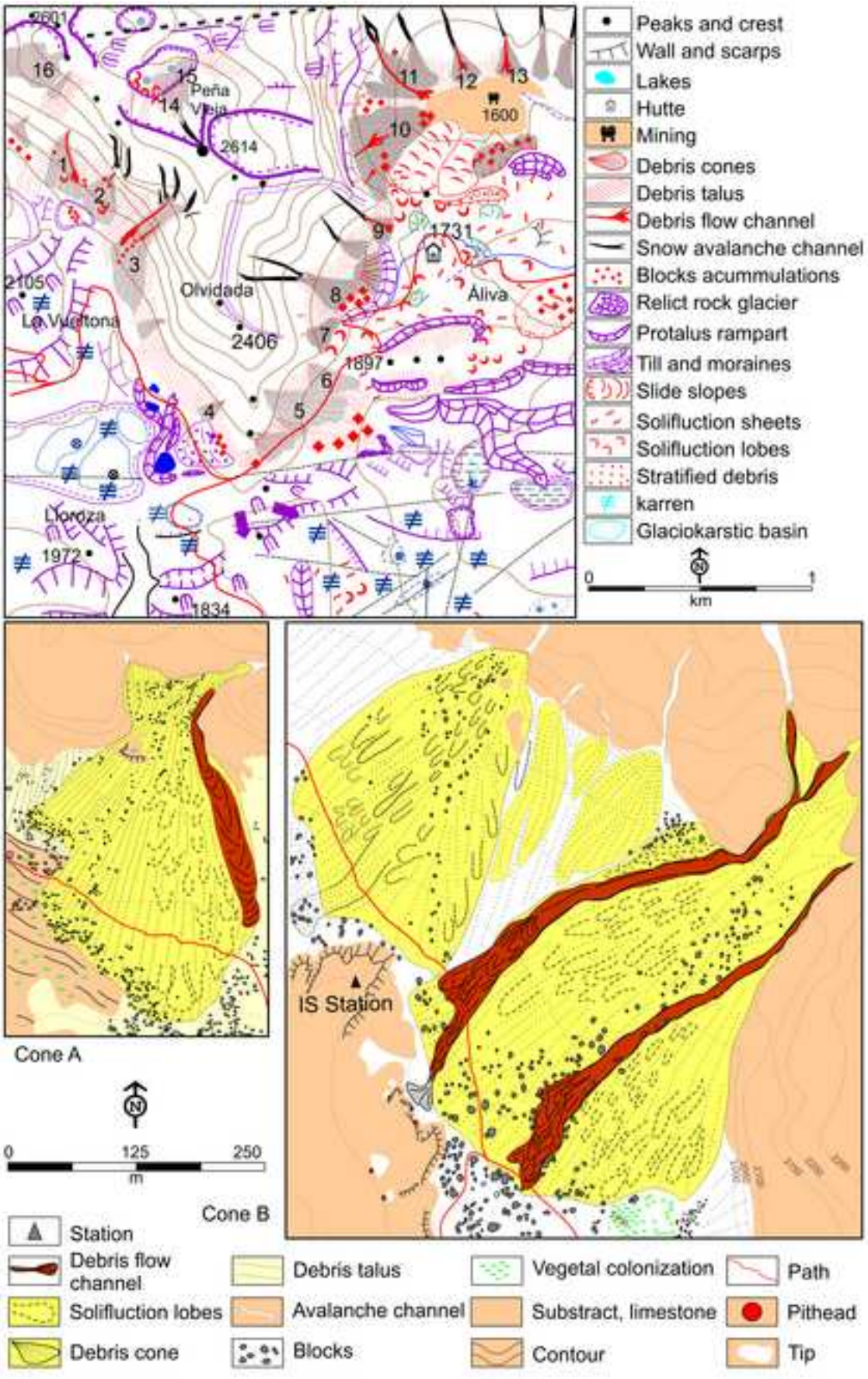

Figure 2. Up, geomorphological sketch of Peña Vieja Group and surrounding. Number 1 is the debris cone A and number 3 is the debris cone B. Down, detailed geomorphological sketch of debris cones A and B.

Figure 3
Click here to download high resolution image

Figure 3. Debris cones in the Peña Vieja Group, where it is perceptible the relation between wall unevenness and cones development. A. Southwest side, La Vueltona area, 1 and 3 are the studied debris cones A and B. B. Southeast side, Áliva area, debris cones have less development than in the other side. C. Cone B, detail of the surface morphology, debris lobes (L), in the central portion, and debris flow features. D. Debris cone B, note the texture of debris flow channel and fan, and the profile with debris lobe (L). Dfc, debris flow channel. Dfa, debris fan. E, detail of debris fan in debris cone B.

Figure 4
Click here to download high resolution image

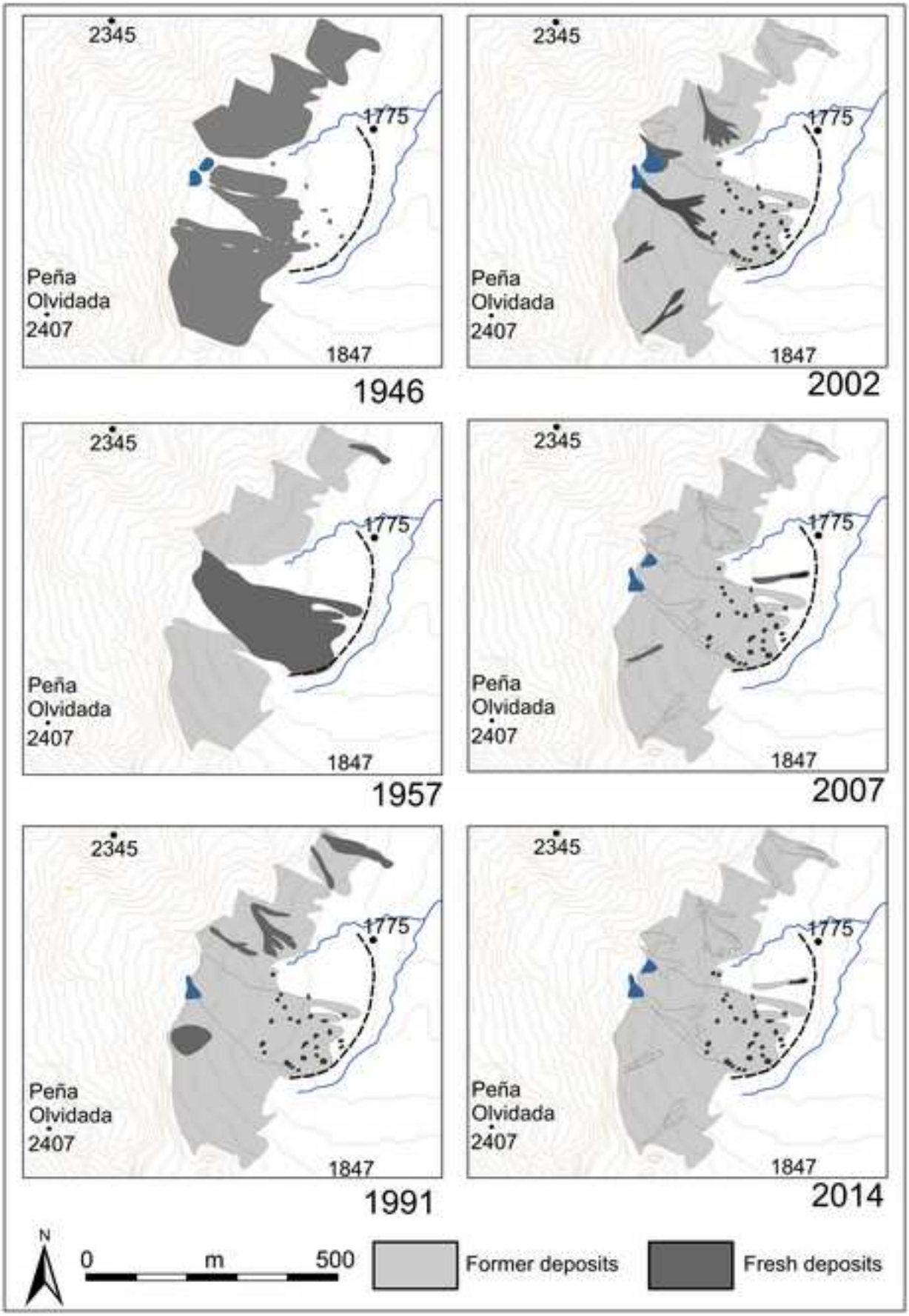

Figure 4. Scree infill in the cirque SE of Peña Vieja-Áliva (1946-2014).

Figure 5

Click here to download high resolution image

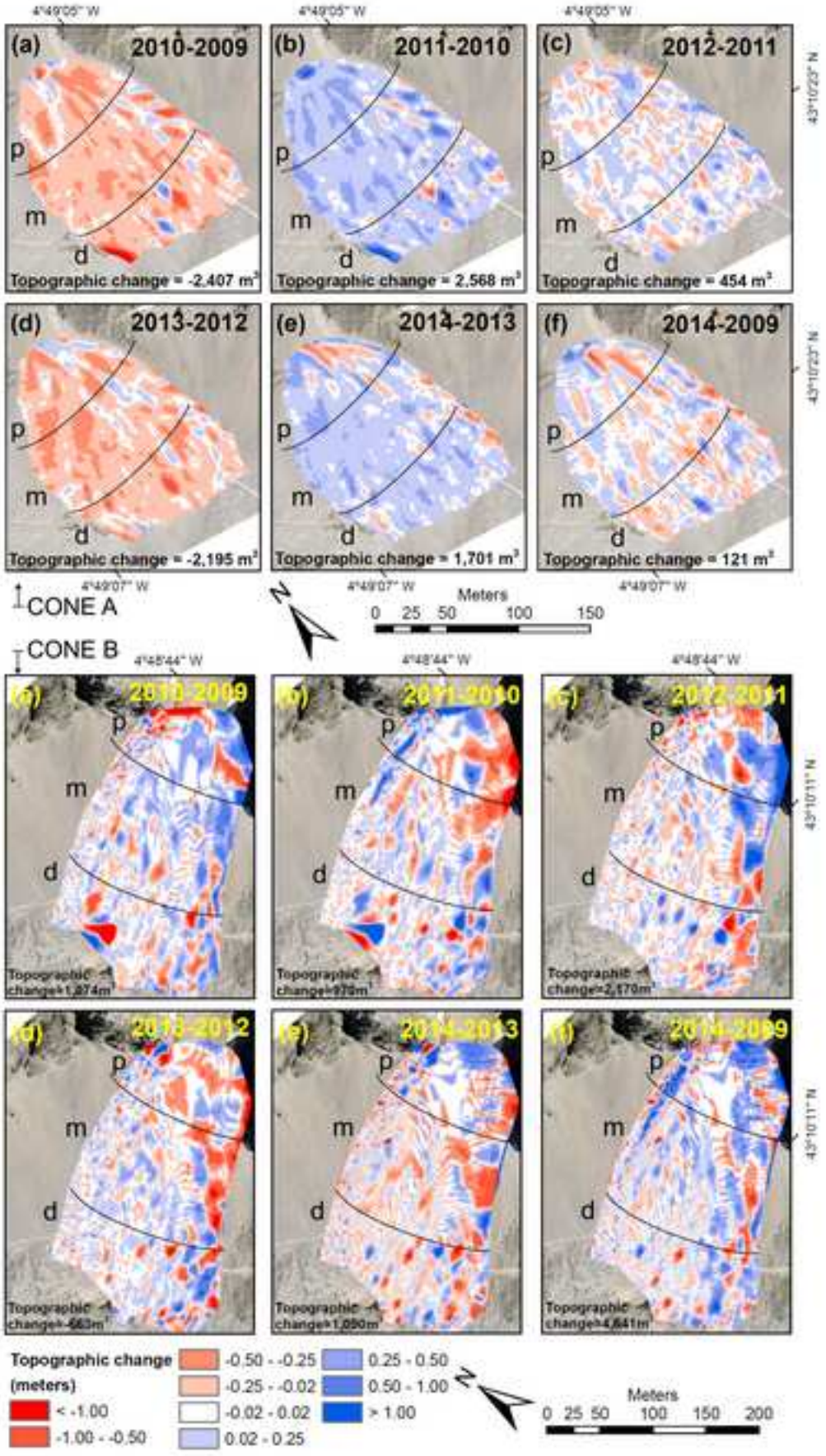

Figure 5. Topographic changes in Cone A (number 1 in Figure 2) and Cone B (number 3 in Figure 2).

Figure 6

Click here to download high resolution image

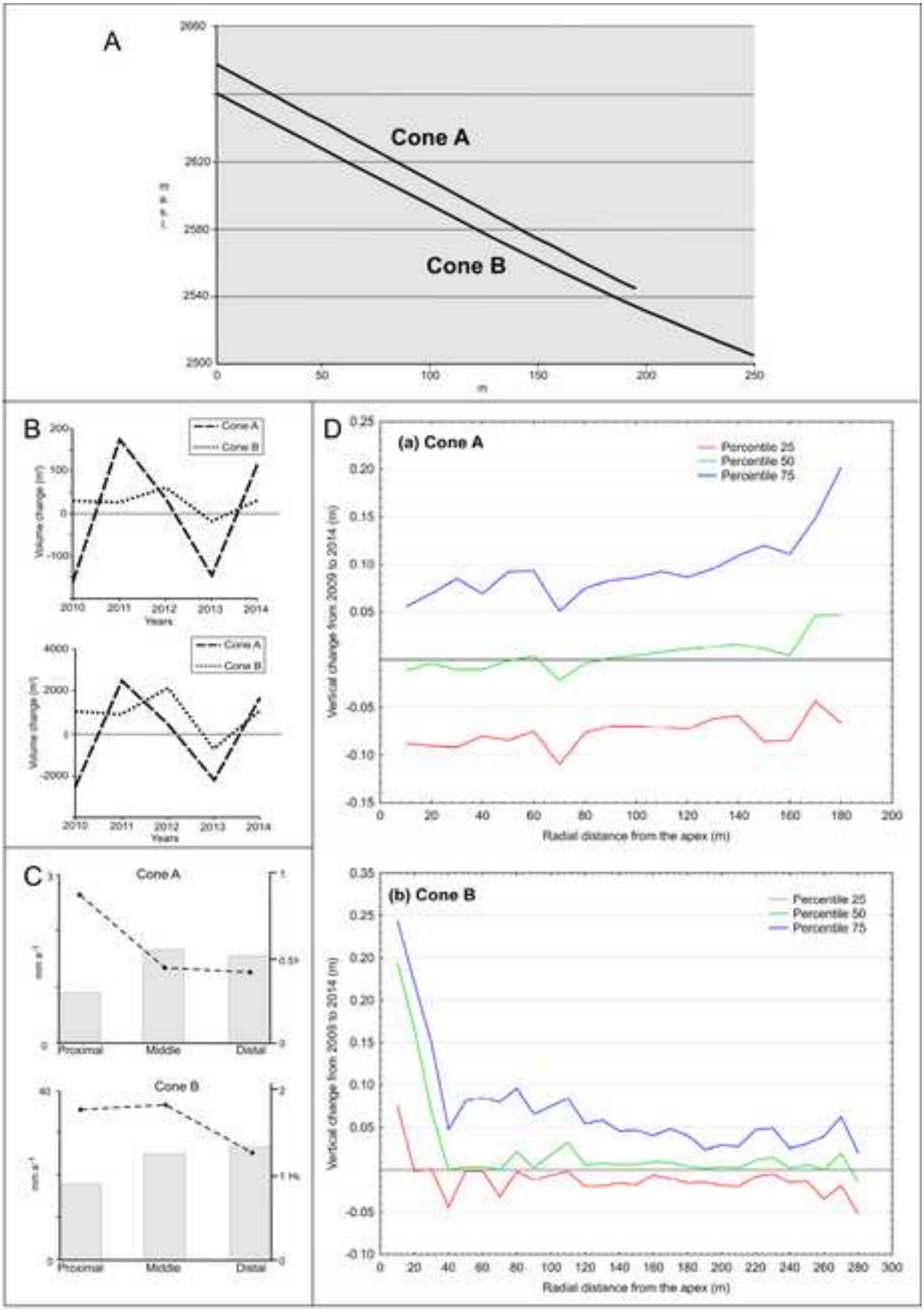

Figure 6. A, profiles of the cones A and B. B, year on year evolution of volume changes (m3) and accumulation rates (mm a-1) in debris cones A and B. C, accumulation rates by parts and surface of debris cones A and B.D, vertical changes at different radial distances from the apex (a) Percentiles 25, 50 and 75 for vertical changes experiences by locations in cone A (a) and cone B (b) at different radial distances from the apex.

Figure 7

Click here to download high resolution image

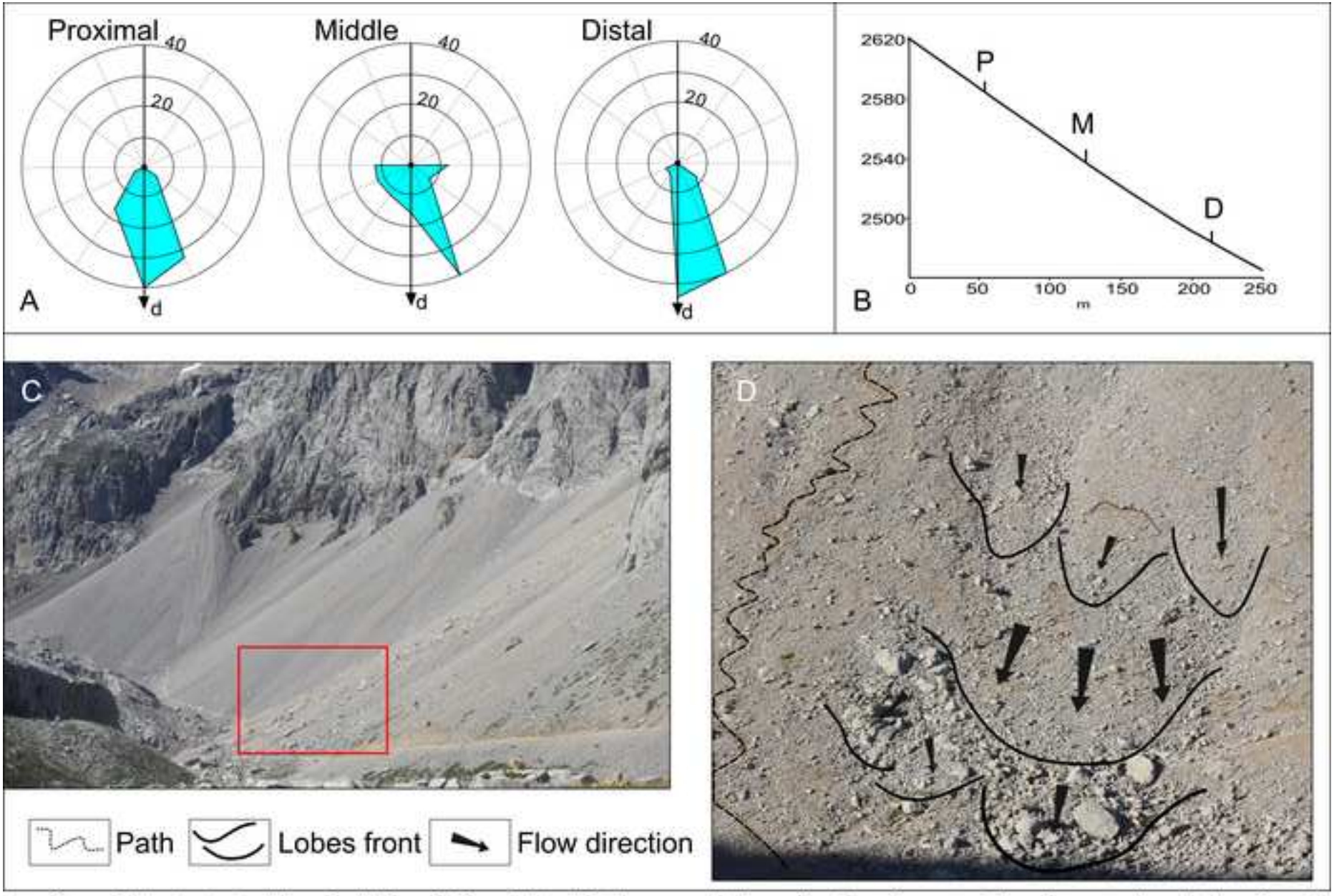

Figure 7. A. Axe L boulder orientations in Cone B by altitude areas. d, slope direction. Representation in percentage. B. Location of represented points in the profile of cone B. C. Slow mass wasting in the distal part of debris cone B. D. Detail of lobes and flow direction where the surface structure visible in TLS diagrams show transversal structures to flow direction.

Figure 8

Click here to download high resolution image

	Wall	Proximal	Middle	Distal
Processes	Rockwall Snow avalanches Frost cracking	Creep Solifluction Debris flow Rockfall	Creep Solifluction Debris flow	Creep Slow slide earthflow Slope wash Setting
Landforms	Walls Avalanche channels	Boulder accumulation Debris lobe Debris flow channels	Debris lobes Solifluction lobes Debris flow channels Small block streams Scattered boulder	Debris fan Debris lobe Planar slide lobes Slide tongues Scattered boulders
Deposits		Rollong boulders Slide boulders Stratified matrix supported Clast supported Diamicton	Rolling boulders Slide boulders Stratified matrix supported Clast supported Diamicton	Rolling boulder Slide boulders Scattered boulders Aligned boulder Clast supported Diamicton

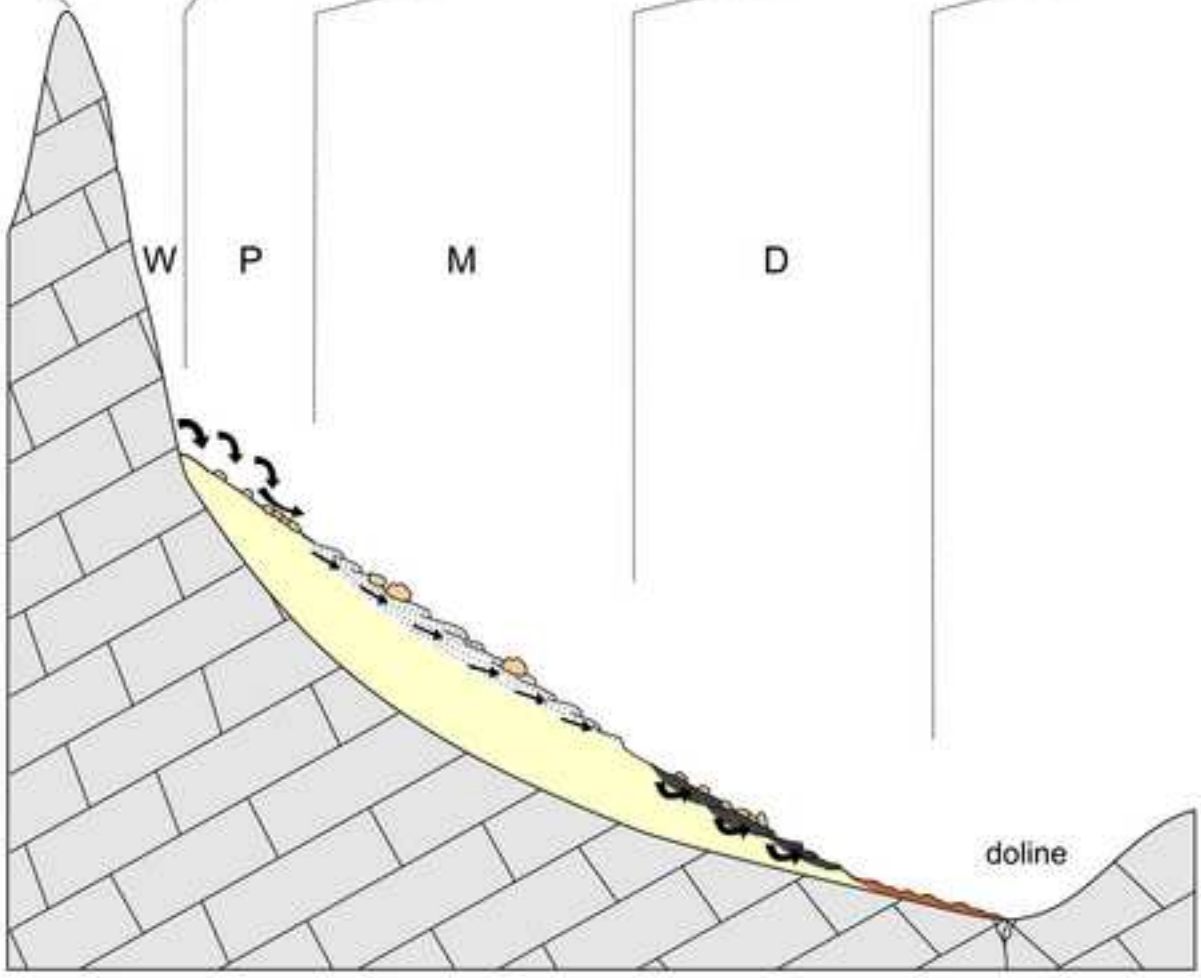

Figure 8. Toposequence of Debris cone B, with representation of processes, landforms and deposits.